

**Transition Radiation Detector
Gas Supply System:
BOX S MECHANICAL STRUCTURE
AMS-02
25/11/2002**

C.Gargiulo*, R.Becker**

*INFN Sezione di Roma

**MIT

§1.Introduction

Box_S mechanical structure's purpose is to position and support the main components of the TRD Gas Supply System in AMS_02. It consists of two large spherical Xenon and CO₂ tanks, a small cylindrical Mixing tank and valves, filters, temperature and pressure sensor, which constitute the gas circuit.

The structure is supported by the AMS_02 Unique Support Structure (USS) (fig.1).

This document provides design development with reference to Document "Box_S Mechanical Structure AMS_02" 15/03/2002.

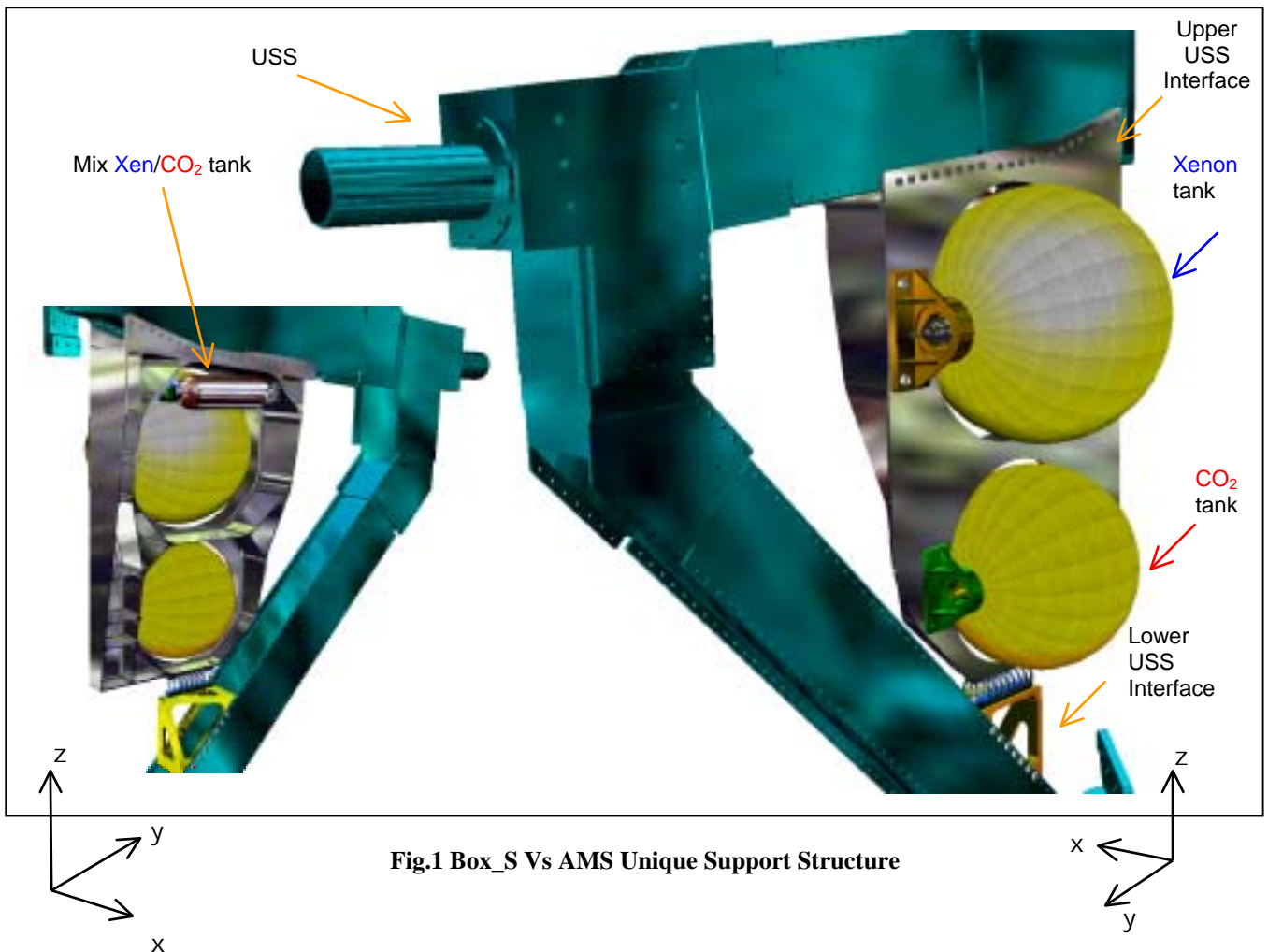


Fig.1 Box_S Vs AMS Unique Support Structure

§2.BOX_S: Conceptual Design

Box_S design was updated according to new definition of the geometry at interfaces, production requirements and finite element analysis results.

§2.1. Gas Tanks

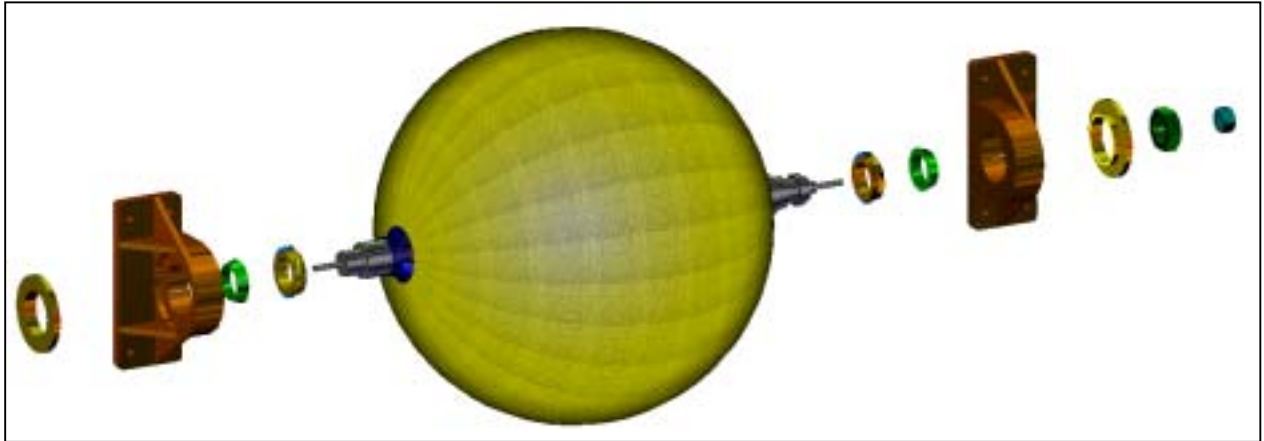


Fig. 2 Xe Tank + Support Brackets (artistic view)

Xenon and CO₂ tanks are spherical composite wound metal shells, roughly 15 and 12 inches in diameter weighing about sixteen and nine pounds. The tanks, designed and built by Arde Inc, are sized to hold 109 pounds of Xenon and 18 pounds of CO₂ respectively (fig.2, 3).

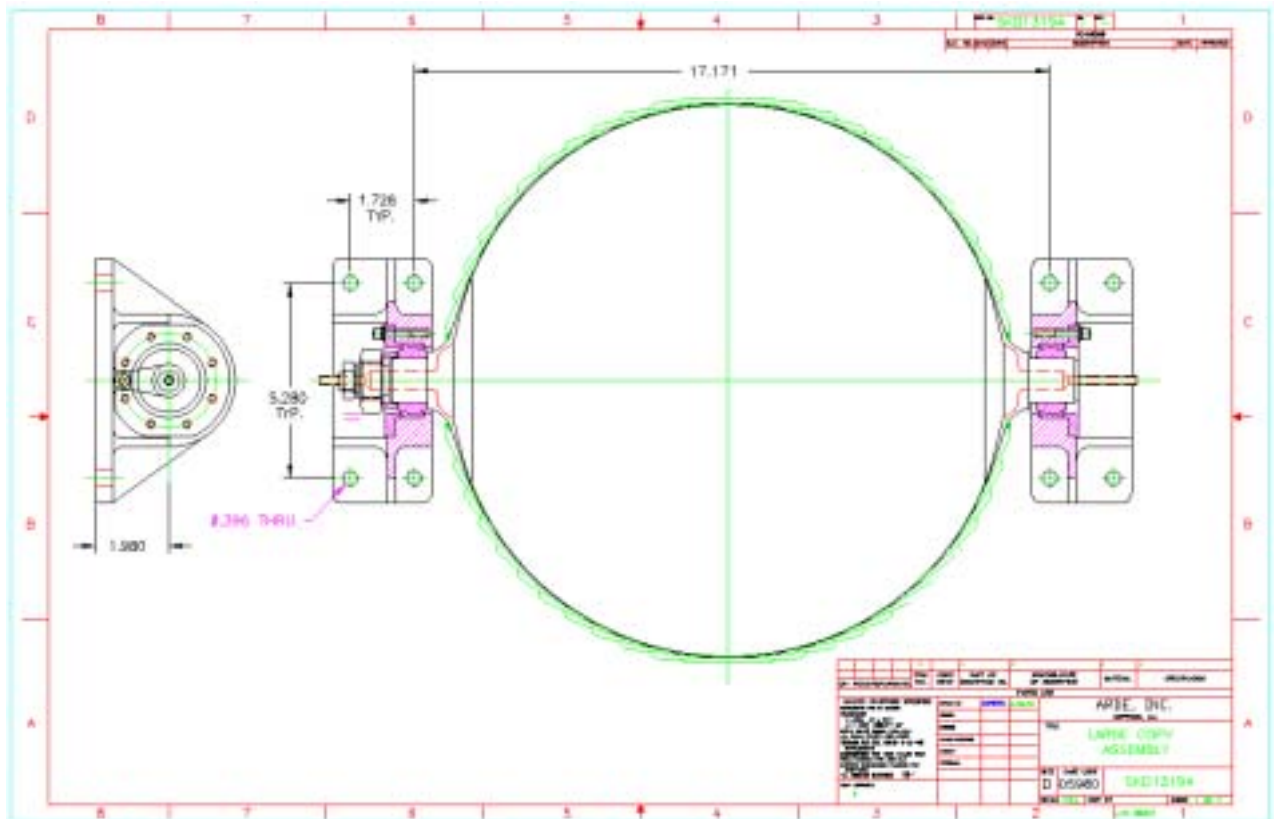


Fig. 3 Xe Tank + Support Brackets (Arde Inc Drawing)

The tanks are fixed to Box_S via a polar mounting; they are supported by bosses cradled in brackets on both ends. One of the bosses is completely restrained and the other is allowed freedom to slide axially, allowing the tank to expand thermally and avoiding introduction of radial loads.

The bearings used at fitting are an Arde Inc aerospace standard production.

The brackets for Xen and CO₂ tanks are made out of Al Alloy 6061 T6. Four screws bolt to the face plate of Box_S.



Arde also manufactures the small stainless steel Mixing tank positioned at the back of the support plate, close to the USS upper trunnion bridge (fig.4). Brackets supporting this tank have a new design finalized to tank new position (fig.5).

One boss of Mixing tank is hard mounted-directly screwed to one (left) bracket, and the other boss is mounted in a bracket having a plastic sleeve that simply support the boss and allows sliding.

Bracket material is Al 7050 T7451 (scratch material from main plate).

Fig. 4 Mixing tank position



Fig. 5 Mixing Tank + Support Brackets

§2.2. Box_S Support Structure

Plate

The support main structure is a light and stiff plate manufactured by milling from a single wrought Al alloy block. The selected material is the wrought aluminum-based zinc-copper-magnesium-content alloy with ANSI designation 7050 T7451 (fig.6).

The Plate's Tank mounting side is planar and has two large holes cut into it that house the Xe and CO₂ tanks.

Ribs behind the front planar face stiffen the structure.

The ribs thickness, starting from 149mm depth at the top and tapering down to 45mm at the bottom give the structure the necessary stiffness. The rib-reinforcement was designed as a symmetrical frame about the centreline from Xe to CO₂ tanks axis, but additional stiffness needed to support local loads for the main (hard mounted) brackets required and additional vertical and corresponding horizontal ribs.

Front plate thickness is 6mm while rib thickness varies from 3 to 5mm.

The predicted relative displacements between upper and lower USS attachment points does not allow a rigid connection at both interfaces without causing a load transfer from the USS to the Box structure. Therefore the design provides a rigid bolted connection at the top and a flexible mount at the bottom. The bottom support has to allow for the large displacements but still contributes stiffening the system. The structure supported only by the upper beam, must satisfy the structural requirements; the additional support at the bottom has to be seen as an additional fail-safe structure.

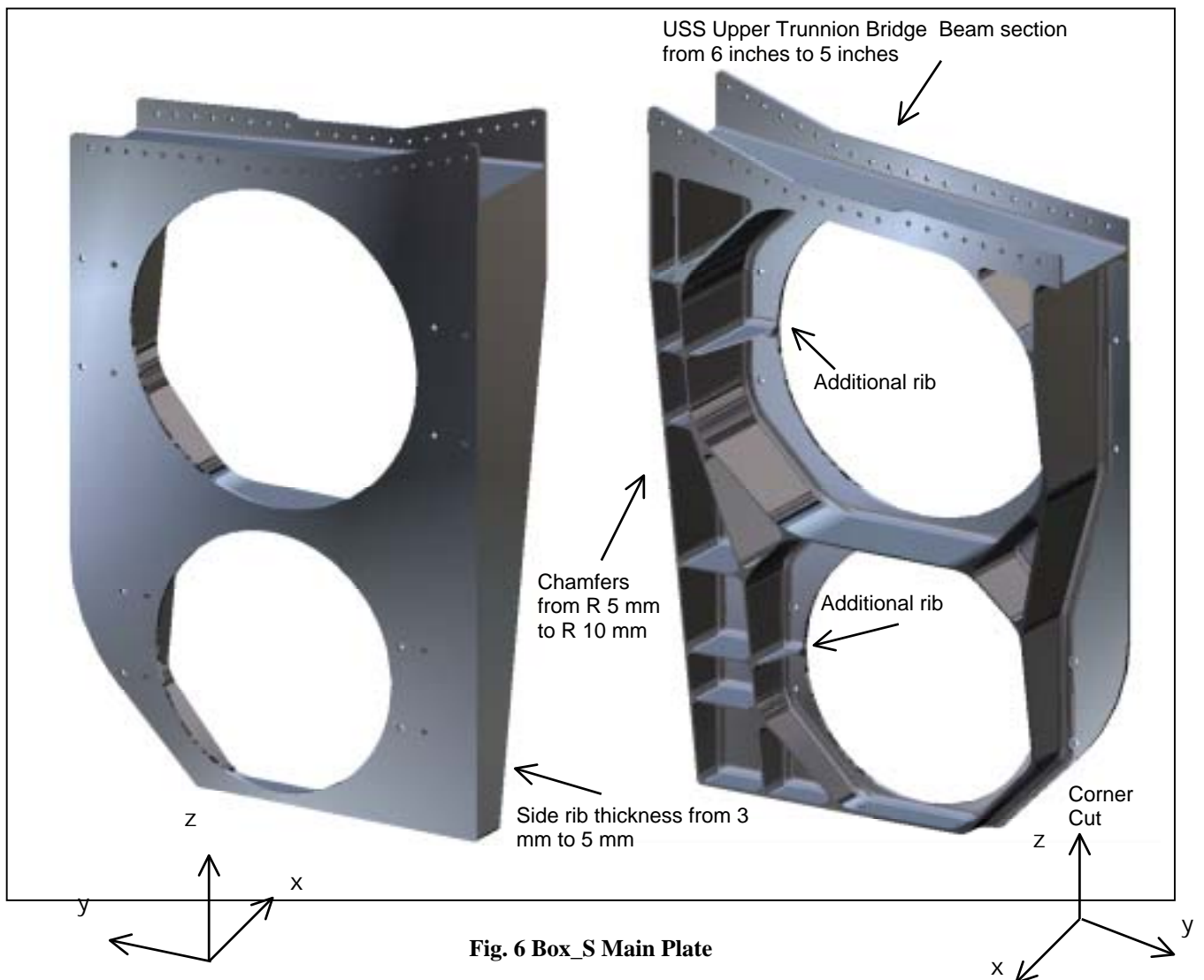


Fig. 6 Box_S Main Plate

Upper Interface with the USS is the U-shape found at the top of the Box that fits outside the upper trunnion bridge and bolts to the USS's standard hole pattern on the lower side of the USS's upper trunnion bridge.

The side plates of the "U-channel" consist of an extension of the frontal main plate on one side and by a 6mm thick section on the other side.

The U-channel width and shape are machined to fit the USS while also allowing installation and USS machining tolerances. Peel-shims are foreseen to fill the over tolerances.

USS Upper trunnion bridge has a transition from the VC-Joint to the Beam. In this transition the section width changes from 142.8750mm to 128.5875mm.

The Box-U-channel precise fits outside the VC-Joint geometry leaving a gap between the Box and the USS Beam. An Al alloy plate shims the gap.

The hole pattern in the USS is copied both at the front and at the back of the Box resulting in a 21, ¼ inch, screws per side that produce the mechanical connection.

Rivet nut bars are placed at the inner side of the USS beam and screws go from the outside of the Box, through the upper trunnion bridge into the self locking rivet nut bars (NAS 1789) (fig.7).

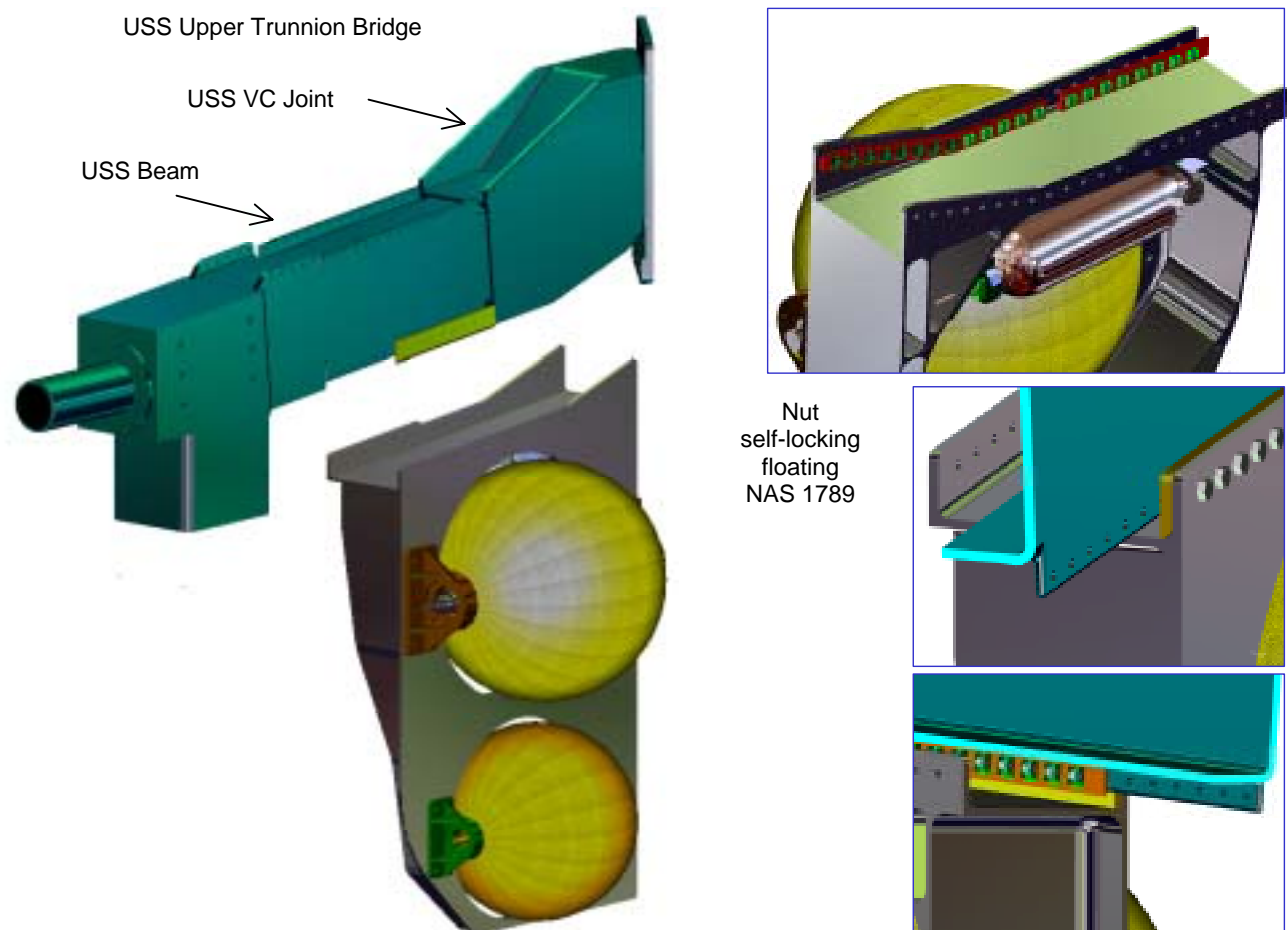


Fig. 7 Box_S / USS Upper connection

Lower Interface with USS consist of a USS hard-mounted triangular aluminum bracket on which a helicoidal stainless spring is attached that in turn is mounted to the box's main plate (this is the flexible mount). The spring is bolted to the Box and USS lower triangular bracket using four M6 screws.

Design updates

Lockheed Martin final decision to reduce the width of USS upper beam from 6 to 5 inches required that the the Box_S geometries be modified correspondgly. Pareticularly to ensure the best fit for the upper USS interface.

The distribution of valves filters and pipes produces a concentration of additional masses mainly at one side of the Box (opposite to tanks main support). This srequired an increase of rib thickness in this area from 3 to 5mm (fig.6).

The front plate lower outer corner, not having any structural function was cut to save weight. An additional rib under the main support for each of the two spherical tanks was intrtruduced for additional stiffner.

The radius of the chamfers in the whole rib reinforcement area was enlarged from 5 to 10mm in order to simplify the production expecially in those areas in which deeper machining is needed.

Material 7075 T6 previously chosen is not reccomended because of stress corrosion problem.

Al 7050 T7451 AMS4050 ref MIL-HDBK-5H was preferred to Al 7075 T7351, not certified in militar standard for thickness over 4.0 inches.

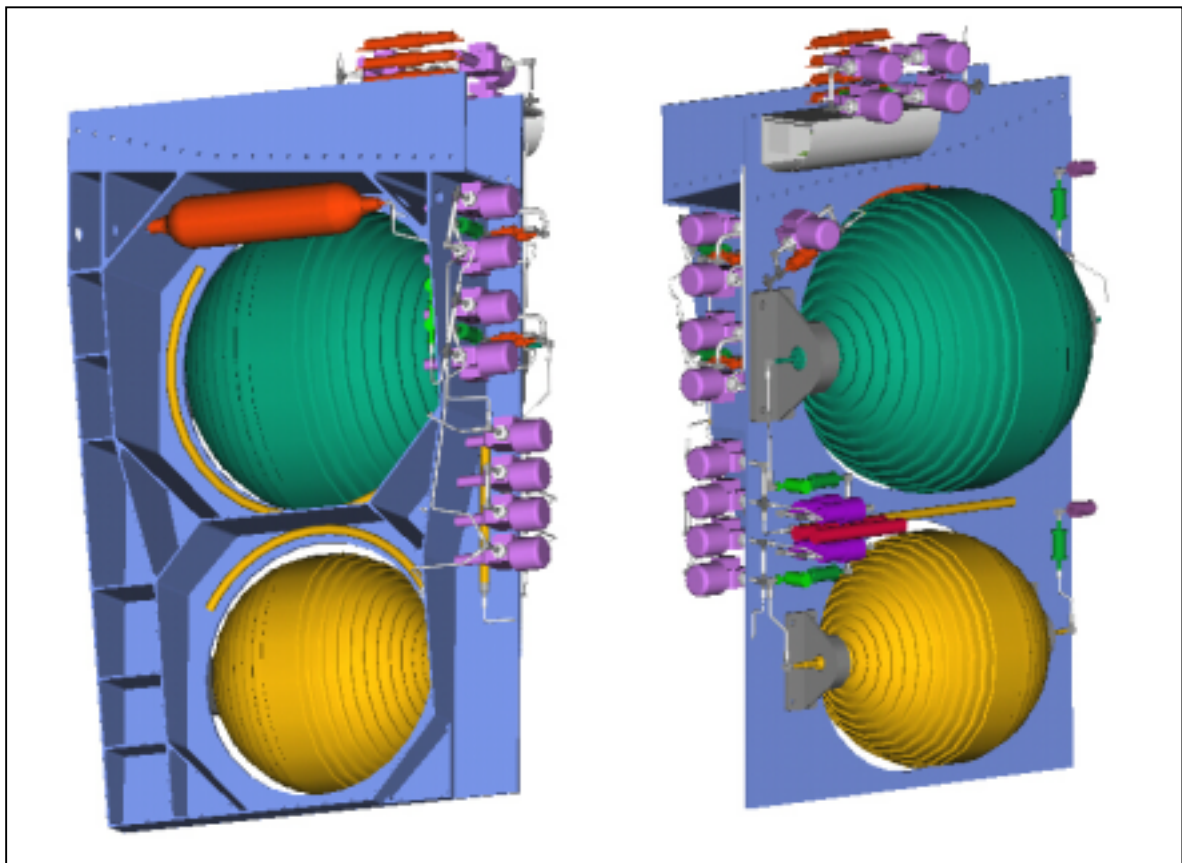


Fig.8 Box_S plumbing

§2.3. Helicoidal spring

The flexible support system at the bottom consists of a helicoidal spring (POWERFLEXH631) (fig.9).

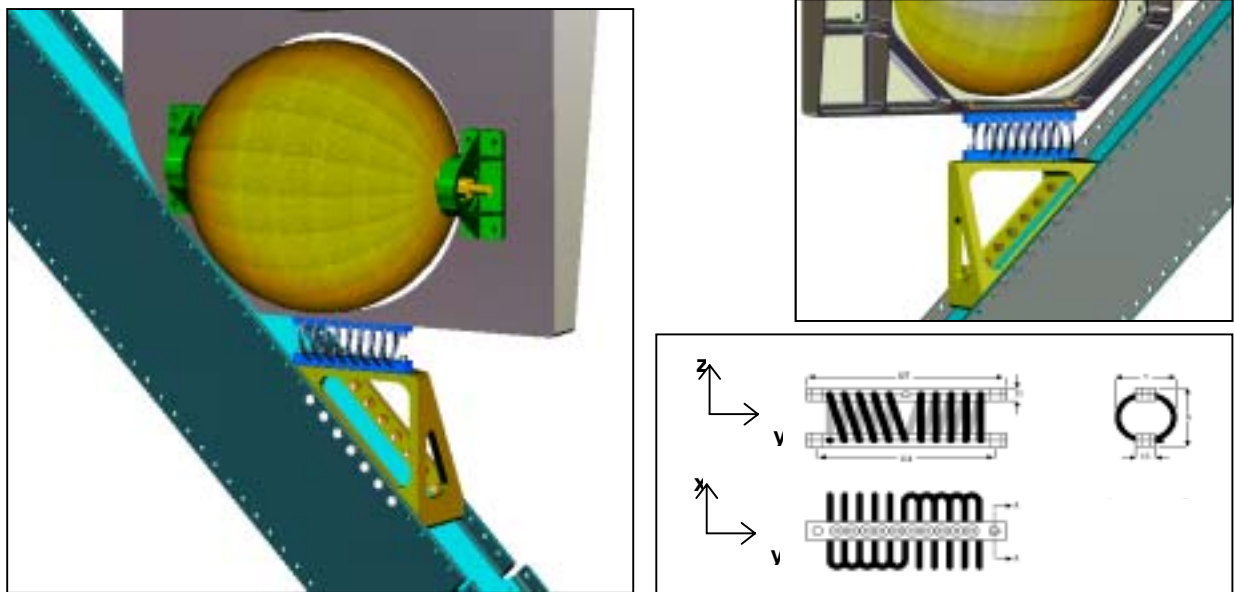


Fig.9 Spring Cables: stainless steel, Bars: stainless steel, Screws: stainless steel

The spring allows for large deformation relative to its size, and introduces a low amplification factor, less than three, at resonance thanks to the viscous damping introduced by the wires strands.

The spring consists in a wire cable wound and fixed in two opposite bars.

Cable, bars and screws are stainless steel 304. Component cleaning and passivation are foreseen according to AMS-QQ-P-35.

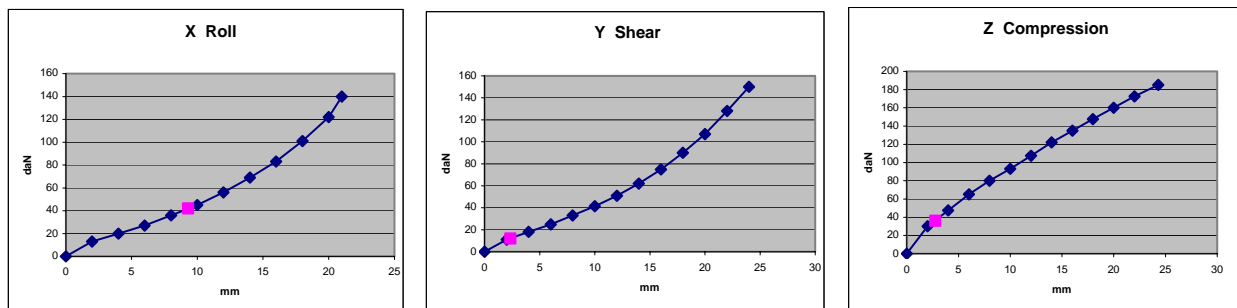


Fig.10 Spring stiffness

Efficiency of spring in term of structure stiffening is limited by its low rigidity necessary to filter the large displacements in the USS. Any reduction in these displacements would allow to increase spring stiffness by modifying wire section and winding.

The non-linear stiffness and predicted working point for the current spring are plotted in fig.10.

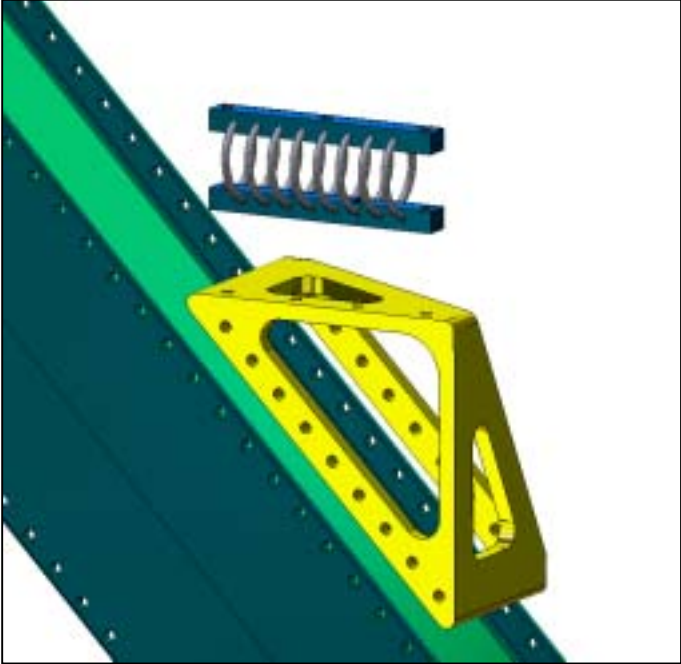
The spring is bolted from one side to the plate by three ¼ inch screws and from the other side to the lower bracket by four ¼ inch screws.

Design updates

All materials changed in to stainless stell 316 amagnetic.

For safety reason, even if predicted reaction are low, the number of bolts necessary to fix the spring to the structures was increased from two to three per side. For spring construction simplification at one side (interface with lower bracket) four through bolts holes were produced instead of three.

§2.4. Lower bracket



Lower triangular bracket bolts to the USS along the hypotenuse side (fig.11). The bracket fits inside the USS and respectively nine bolts at the front and nine at the back connect the two. Four holes at the top of the bracket house the bolts for the connection to the spring. The bracket is manufactured from Al 7050 T7451 (scratch material from plate production).

Design updates
Based on low stress level predicted at the lower bracket, the design was optimized in order to reduce the weight.

Fig.11 Lower bracket design

§3.Box S: Structural Analysis

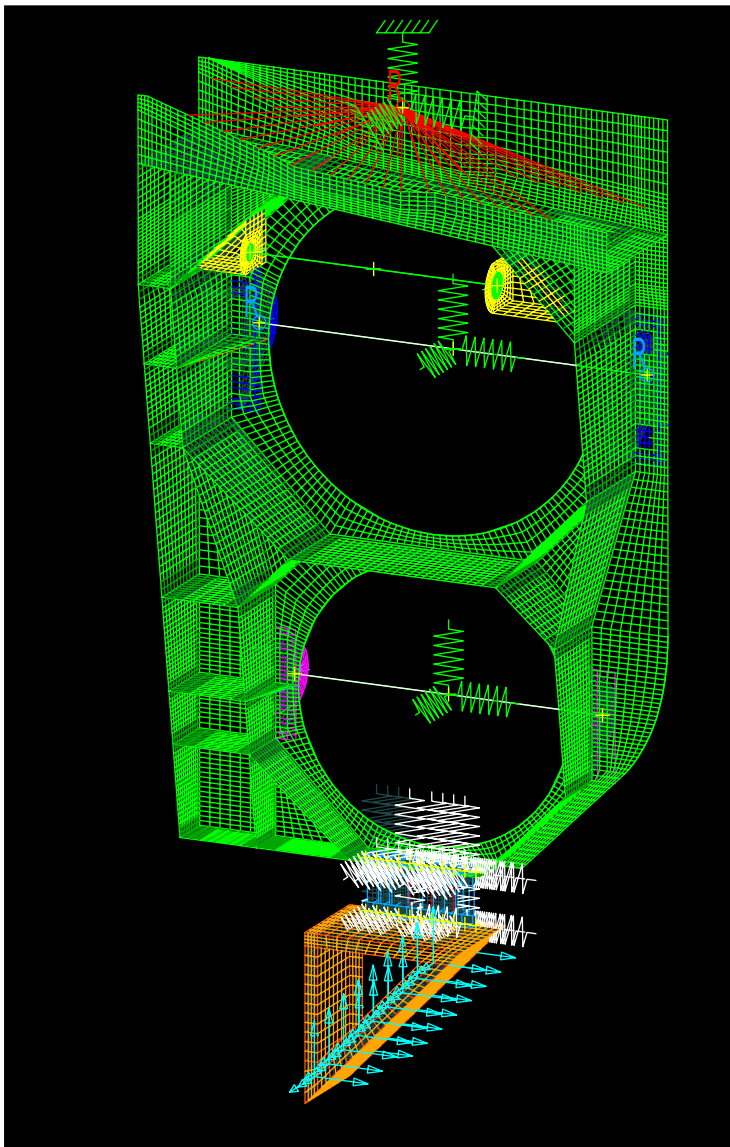


Fig.12 Box_S: FE mesh

A finite Element Analysis was performed to evaluate Box_S static behavior in term of displacement, stresses and reactions at structures interfaces under critical load conditions that primarily occur during launch and landing.

A modal analysis was carried out to verify that the first significant structure natural frequency is above 50 Hertz.

§3.1. Finite element model

Box_S is completely mapped meshed (fig.12).

Plate is modeled with shell elements Mindlin theory based. The plate chamfers are taken in to account by increasing corresponding element thickness (fig.13).

The final stiff design of the tanks brackets is introduced in the model (fig14, 15).

The helicodal spring at the lower attachment points modeled by two linear beams simulating the two bars and by eight rigid bars with extreme nodes coupled to beams nodes by rotational and translational spring simulating the spring coils.

Tanks are modeled as lumped mass in their center of mass and are connected to the brackets by rigid bars whose extreme nodes are properly coupled with bracket bearing node.

The considerable weight of Xenon compared to tank required some consideration on the property of the Xenon and its behavior under vibration.

Model assumptions are based on hypothesis that, during critical load phases, Xenon is single phase and incompressible, and tank is very rigid.

This last hypothesis due to tank constrain vs. brackets brings to higher frequency for lateral mode (x, z) of the system tank+brackets, and only partially affects the axial mode.

Regarding assumption on the interaction of Xe and vessels, the fluid is assumed single phase (above 47F), at launch and therefore doesn't slosh [Document EID-02322-1]. Launch significant loads where assumed to occur at Space Shuttle Cargo bay (temperature control around 70F to 85F) with Xenon occupying the entire tank volume.

Single phase Xenon supports acoustic modes. From previous analysis [Document EID-02322-1] it is known that only first diametral mode is expected to interact significantly with the structure. Predicted natural frequency of Xe at 70F is 424Hz.

Proximity of the first diametral acoustic mode with any translational mode of the tank would result in a significant coupling of the structure and fluid and resulting increased in boss loads. But tank+brackets natural frequencies are significantly lower and mounting the bracket on Box_S reduces this frequency even more due to flexibility of the Box. So Xenon appear fair stiff relative to the tank. Based on that, the incompressible Xen assumption is quite accurate. The same simple assumptions were made in analysis of the CO₂ tank, in this case two phase conditions only occurs during discharge of CO₂ that doesn't occur during launch.

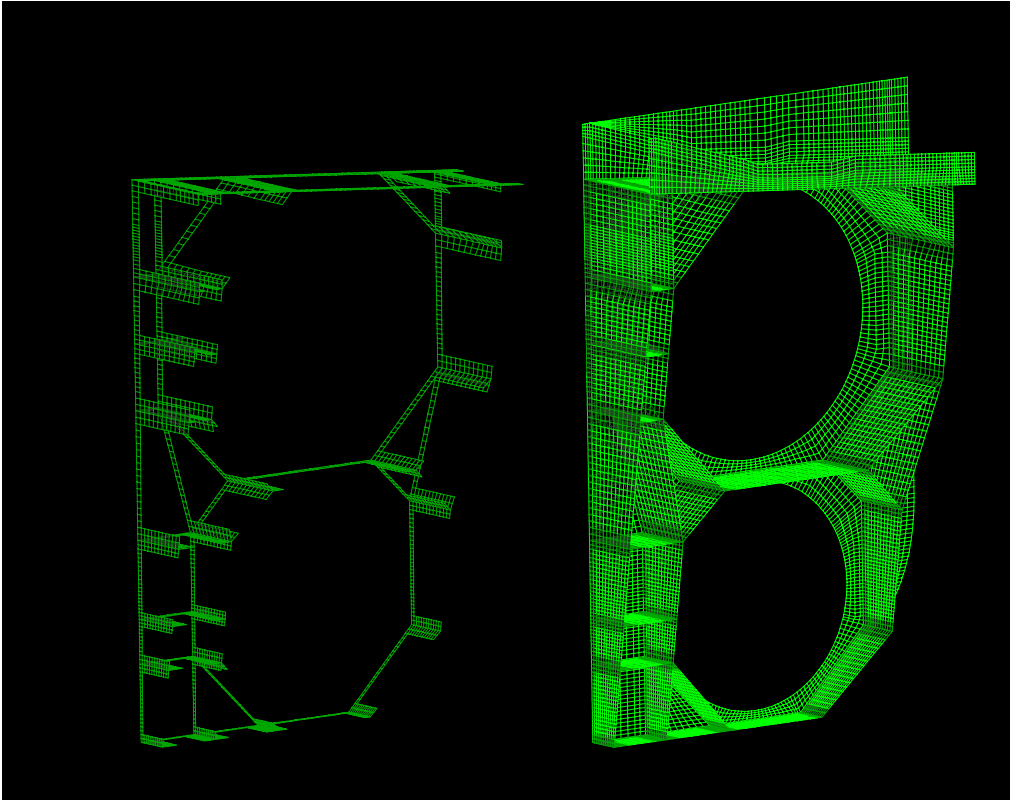


Fig.13 Box_S: Plate FE mesh, Plate reinforcement detail

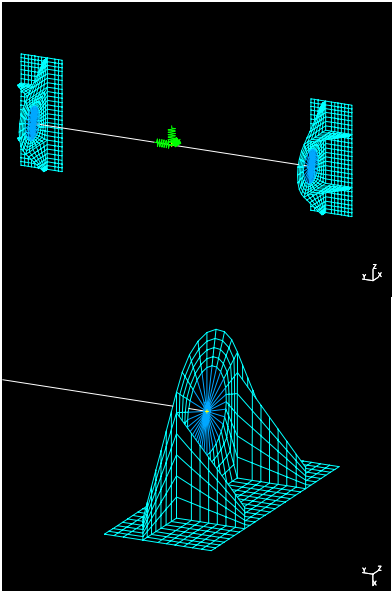


Fig.15 Tank brackets mesh

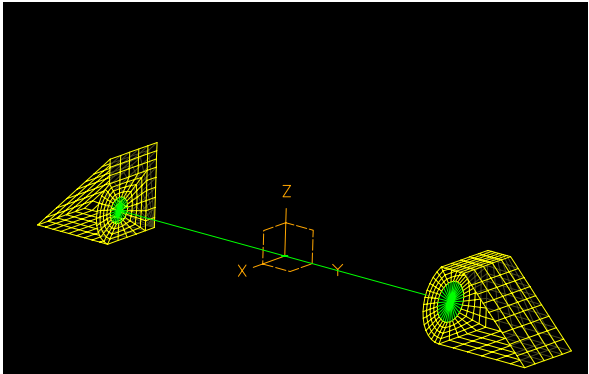


Fig.14 Mixing tank brackets mesh

§3.2. Type of element used

I-deas: 94 thin shell, 161 lumped mass, 121 rigid bar, 23 rigid element, 2 linear beam

§3.3. Applied units

Length [mm], Mass [g], Force [N].

§3.4. Type of material used

Plate, Lower bracket, Mixing tank brackets

Al Alloy 7050 T7451

$\rho=0.0028 \text{ g/mm}^3$ $E = 71000 \text{ N/mm}^2$ $\nu = 0.33$
 $F_{ty}= 386.1 \text{ N/mm}^2$, $F_{tu}=455 \text{ N/mm}^2$, $S_u= 303.4 \text{ N/mm}^2$

Xen and CO2 brackets

Al Alloy 6061 T6

$\rho=0.0027 \text{ g/mm}^3$ $E = 73000 \text{ N/mm}^2$ $\nu = 0.33$
 $F_{ty}=240 \text{ N/mm}^2$, $F_{tu}= 290 \text{ N/mm}^2$, $S_u= 186 \text{ N/mm}^2$

Helicoidal spring

Stainless steel 316

$\rho=0.0081 \text{ g/mm}^3$ $E = 193000 \text{ N/mm}^2$ $\nu = 0.29$
 $F_{ty}=240 \text{ N/mm}^2$, $F_{tu}= 550 \text{ N/mm}^2$, $S_u= 340 \text{ N/mm}^2$

§3.5. Constraints and Loads

Constraints:

Screws connecting Box and USS are modeled constraining translations and rotations at corresponding nodes.

Screws connecting the tanks brackets to the plate are modeled by coupling the node Degree Of Freedom of the different parts at screws location.

At the tank main supporting bracket all translations and the rotation relative to the tanks polar axes are coupled with the bracket central node that simulate the bearing (X, Y, Z translational and Y rotational DOF coupled, X and Z rotational DOF free).

At the other boss of the tanks only translations normal to the polar axis are coupled to bracket bearing node (X, Z translational DOF coupled, all the other DOF are free).

Loads:

The load cases considered are the Box_S mass subjected to an acceleration vector and combined with imposed relative deflection between attachment points.

Acceleration imposed:

$\pm 13g$ in one direction with $\pm 3,25g$ simultaneously applied in the other two directions according to Document JSC-28792; different load cases were considered by sweeping the direction of the acceleration vector.

Displacement imposed:

(9.301; 2.350; 2.746) mm imposed at lower attachment points with USS (fig.16- tab.1)

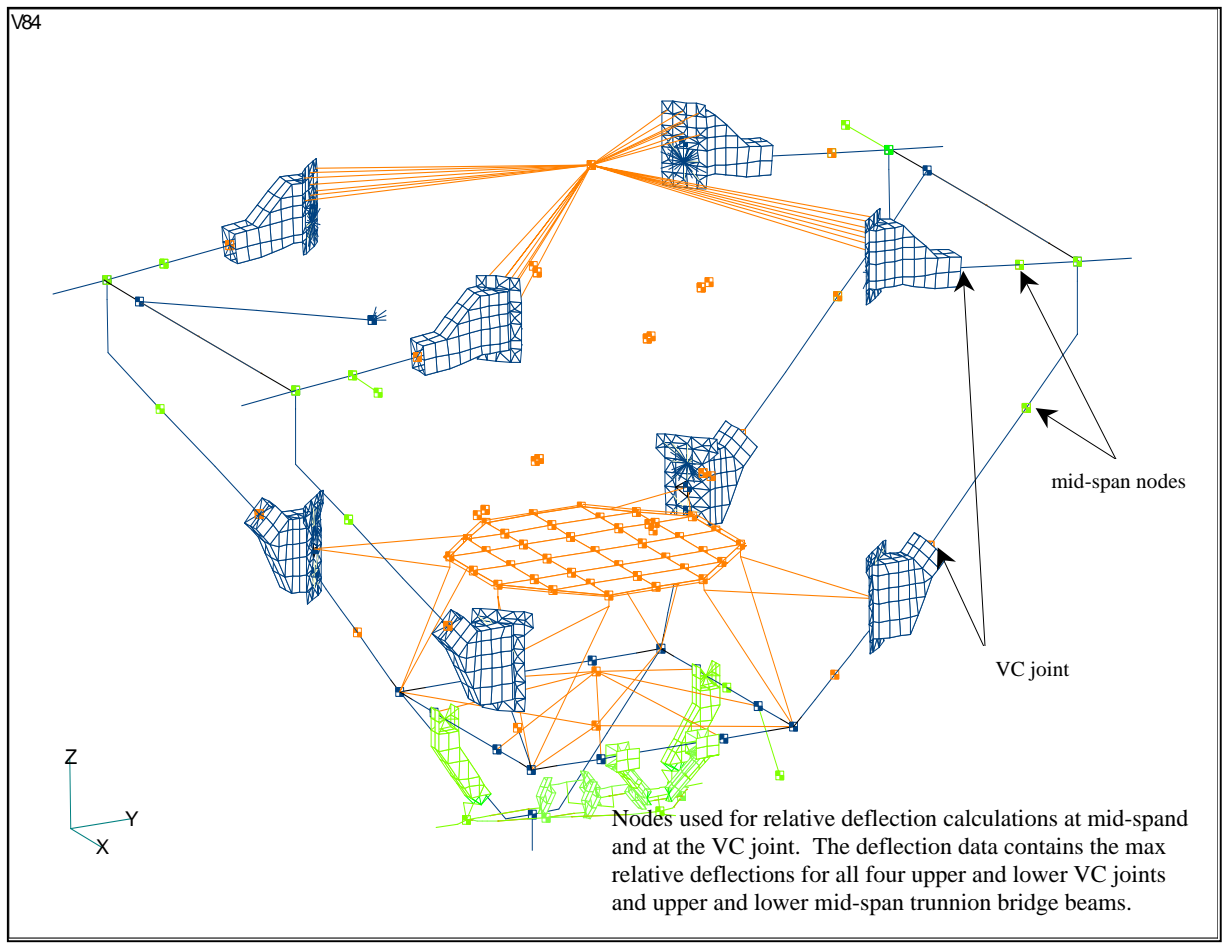


Fig .16: TRD Gas Supply on the USS-02 Model (Lockheed)

Location	Max x Def (mm)	Max y Def (mm)	Max z Def (mm)
TRD GAS supply Midspan	4.514	1.354	1.778
TRD GAS supply VC Joint	9.301	2.350	2.746
All Midspans	5.994	1.481	1.836
All VC Joints	10.640	2.466	3.678

Table1: Relative Deflection results

§3.6. Static analysis: stresses, displacements and reactions

Box_S predicted static behavior satisfies safety requirements.

The calculated stress levels and displacement under different load cases are summarized in tab.2 for each structural component. Yield and Ultimate Margins of Safety (MS) are listed in the same table.

$$MS_{yield} = \frac{Yield\ Stress}{FS_y \times Limit\ Stress\ (Von\ Mises)} - 1$$

$$MS_{ult} = \frac{Ultimate\ Stress}{FS_{ult} \times Limit\ Stress\ (Max\ Principal)} - 1$$

with $FS = Factor\ of\ Safety$

$$FS_y = 1.25 \quad FS_{ult} = 2$$

The reaction forces at the location of the bolts fixing tank brackets to Box and Box to USS are given in tab.3. Reported are Forces [N] per node where each screw is modeled by one node. Reaction distribution in the plate can be appreciated in fig.24-27.

The high reactions must be related to the conservative assumptions made both in the high load level applied and in modeling one screw as one node

Maximum stresses, largest displacements and highest reactions values occur at different locations under different load cases (fig.17-27).

Plate and Xenon tank main brackets are the structures most stressed and in which largest displacements occur.

Load cases (± 13 , ± 3.25 , ± 3.25)g + imposed displacement (9.301, 2.350, 2.746)mm

When the main acceleration component (13g) is normal to the plate in the x positive or negative direction, Xe and CO2 tank mass inertial action produces a plate bending with maximum sag at the bottom. The sag, according to the direction of the acceleration, reaches its maximum value for x negative acceleration (-13g) when displacement at the bottom rises to 1.45mm (fig.17).

Stress concentration ($157\ N/mm^2$) is localized at one side of the back reinforcement close to the back plate that connects the Box to the USS upper trunnion bridge (fig.18).

Largest reactions occur at the side bolts in the upper interface at the back of the U-channel (fig.25, tab.3).

A positive effect of the spring at the bottom is observed when acceleration is in the positive direction, same direction of imposed displacement, when a portion of the bending moment is opposed by the spring; this results in a reduction of reactions intensity at upper screws location (fig.24, tab.3).

Load cases (± 3.25 , ± 13 , ± 3.25)g + imposed displacement (9.301, 2.350, 2.746)mm

When acceleration is mainly in the tanks axial direction, y positive or negative, the Xe tank main bracket is the most loaded. It is there that maximum displacements are predicted (0.774mm for +13g, 0.930mm for -13g) while maximum stress value occurs at the plate in the underlying area ($149\ N/mm^2$, Von Mises, for +13g; $216\ N/mm^2$, MaxPrincipal, for -13g) (fig.19-22).

Largest reactions occur both at bolts fixing the main support for the Xe-tank to the Plate and at the upper Interface of the plate to USS (+3.25,+13,+3.25) (fig.24, tab.3) .

Load cases (± 3.25 , ± 3.25 , ± 13) g + imposed displacement (9.301, 2.350, 2.746)mm
Acceleration main component in z direction has the minor impact on the structure in term of stress and displacement (fig.27, tab.3).

§3.7. Fail Safe Analysis

A fail-safe analysis at the upper and lower USS-02 interface with the highest loaded fastener removed was performed and all Margin of Safety were recalculated. The Factor of Safety used for fail-safe analysis was 1.0 for both yield and ultimate.

For load case (-13, -3.25, -3.25)g bolt n_o. *Plate/Upper interface back_21* (fig.23) at the upper USS interface was removed and behavior recalculated.

Von Mises stress rises from 157 to 184 N/mm² well inside MS and reaction at the adjacent bolt (bolt n.Plate/Upper Interface Back 20) increases about 70% : Bolt MS= 0.378 (fig.28, 29; tab.4,5).

For load case (3.25, 13, 3.25)g two critical cases were considered:

Bolt n_o *Plate/Xen Bracket_4* was removed. Stress under bracket lightly increases staying within safety margins while maximum reaction value increase of about 35% with a new distribution on the other bolts of the same bracket: high loaded bolt MS= 1.006 (fig.30, 31; tab.4, 5).

Bolt n_o. *Plate/Upper interface front12* was removed. Recalculated stress level and bolts reactions produce MS values in the requirements.

Load case (3.25, 3.25, 13)g was considered for the fail-safe analysis of the lower bracket

The reaction at bolts in the Lower Bracket are low under all different load conditions (fig.24-27; tab.3,) due to relative light stiffness of the helicoidal spring necessary to filter the large displacement between attachment points. In any case the highest loads are predicted for this load case. Removing highest loaded fastener bolt. n. *Lower_bracket/USS lower interface front1* brings to an increasing of 10% in maximum reaction value that occurs at the adjacent bolt: MS=1.676 (fig.28, 29; tab.4,5).

RESTRAINTS:					
Upper USS clamped			Lower USS displaced		
Ux	Uy	Uz	Ux	Uy	Uz
0	0	0	9.301	2.350	2.746

LOADS:			PLATE				
Acceleration (g)			Limit Stress [N/mm ²]		Max Displacement [mm]	Margin of Safety	
x	y	z	Von Mises	Max Principal		Yield	Ultimate
13	3,25	3,25	132	142	0.755	1.34	0.60
3,25	13	3,25	149	122	0.618	1.07	0.86
3,25	3,25	13	91	98	0.360	2.39	1.31
-13	-3,25	-3,25	157	140	1.450	0.97	0.63
-3,25	-13	-3,25	189	216	1.100	0.63	0.05
-3,25	-3,25	-13	87	101	0.574	2.55	1.25

LOADS:			Xen BRACKET				
Acceleration (g)			Limit Stress [N/mm ²]		Max Displacement [mm]	Margin of Safety	
x	y	z	Von Mises	Max Principal		Yield	Ultimate
13	3,25	3,25	53	60.4	0.530	2.62	1.40
3,25	13	3,25	60	51.8	0.774	2.20	1.80
3,25	3,25	13	37	42.1	0.316	4.19	2.44
-13	-3,25	-3,25	21	21.5	0.480	8.14	5.74
-3,25	-13	-3,25	65	57.3	0.930	1.95	1.53
-3,25	-3,25	-13	36.7	30	0.330	4.23	3.83

LOADS:			CO ² BRACKET			
Acceleration (g)			Limit Stress [N/mm ²]		Margin of Safety	
x	y	z	Von Mises	Max Principal	Yield	Ultimate
13	3,25	3,25	9.89	9.75	18.41	13.87
3,25	13	3,25	26.1	26.1	6.36	4.56
3,25	3,25	13	7.52	7.56	24.53	18.18
-13	-3,25	-3,25	6.7	5.24	27.66	26.67
-3,25	-13	-3,25	27.3	25.7	6.03	4.64
-3,25	-3,25	-13	7.17	6.58	25.78	21.04

LOADS:			Mixing BRACKET			
Acceleration (g)			Limit Stress [N/mm ²]		Margin of Safety	
x	y	z	Von Mises	Max Principal	Yield	Ultimate
13	3,25	3,25	24	16.8	11.87	12.54
3,25	13	3,25	15	16.7	19.59	12.62
3,25	3,25	13	25.7	27.7	11.02	7.21
-13	-3,25	-3,25	24.8	28.3	11.45	7.04
-3,25	-13	-3,25	15.2	12.7	19.32	16.91
-3,25	-3,25	-13	26.4	29.9	10.70	6.61

LOADS:			Lower BRACKET			
Acceleration (g)			Limit Stress [N/mm ²]		Margin of Safety	
x	y	z	Von Mises	Max Principal	Yield	Ultimate
13	3,25	3,25	34.6	38.7	7.93	4.88
3,25	13	3,25	43.5	43.5	6.10	4.23
3,25	3,25	13	45.5	45.2	5.79	4.03
-13	-3,25	-3,25	47.3	52.1	5.53	3.37
-3,25	-13	-3,25	48.3	49.8	5.40	3.57
-3,25	-3,25	-13	42.5	45.7	6.27	3.98

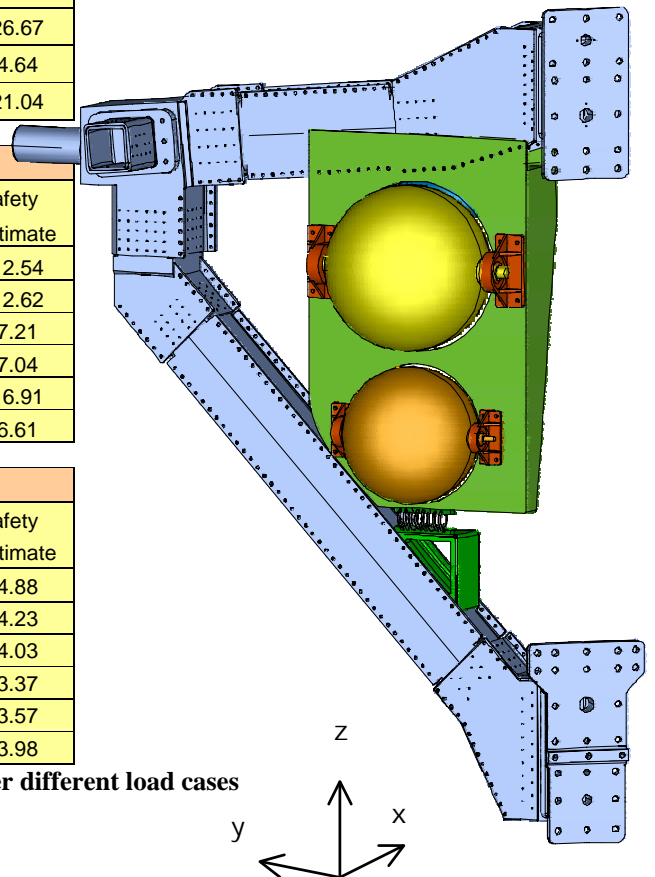


Table 2 Stresses, Displacements and Margin of Safety under different load cases

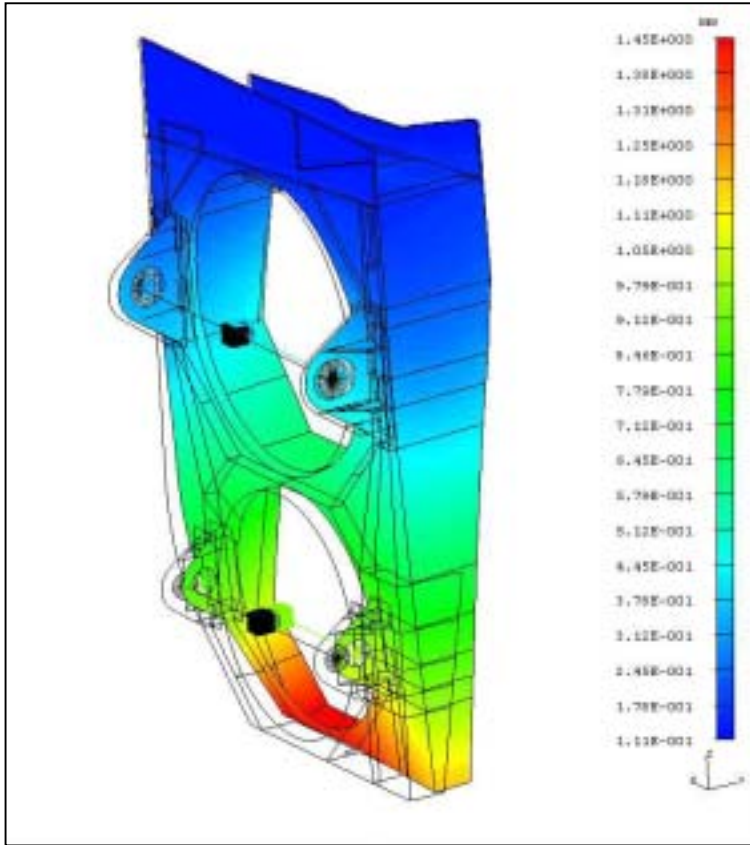


Fig.17 Plate Displacement (Lower Bracket and Helicoidal Spring hidden); load case (-13, -3.25, -3.25) g

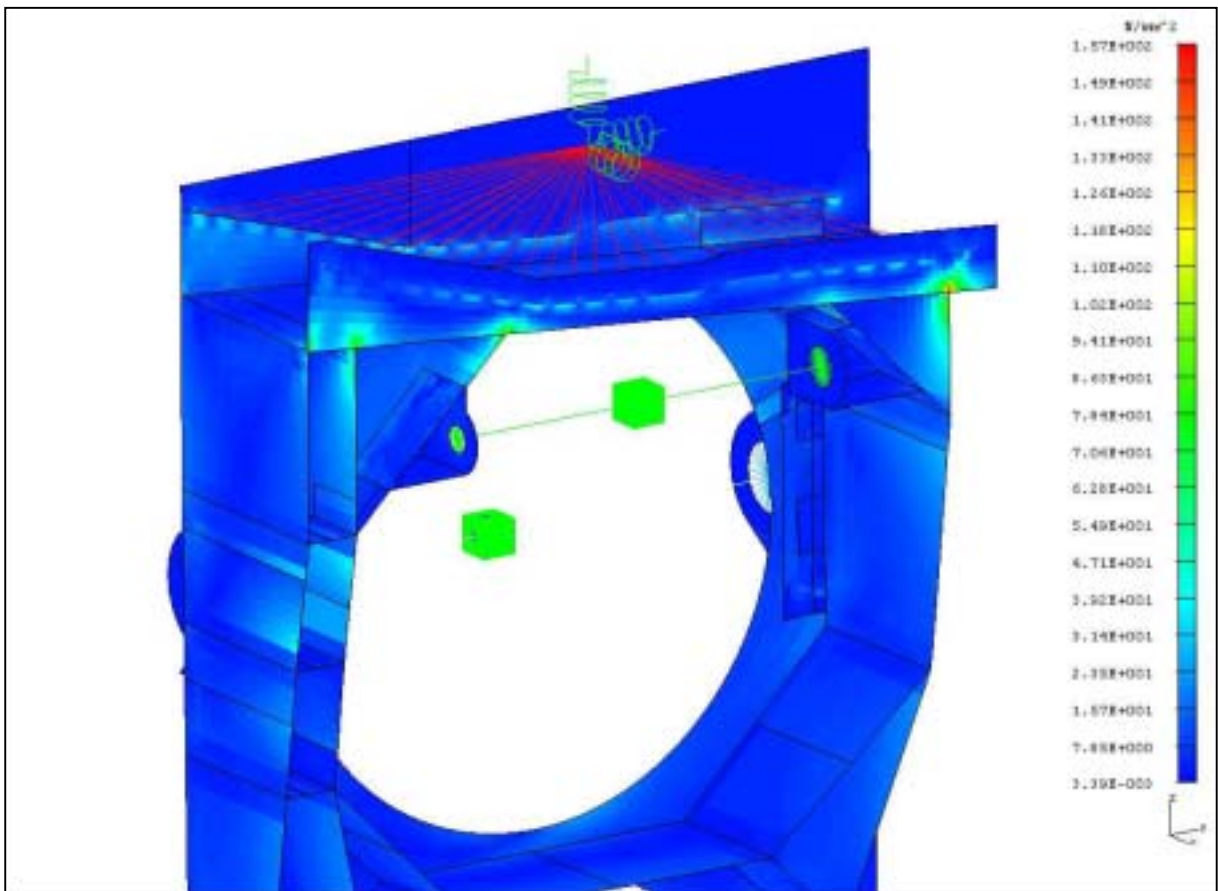


Fig.18 Plate Stress; load case (-13, -3.25, -3.25) g

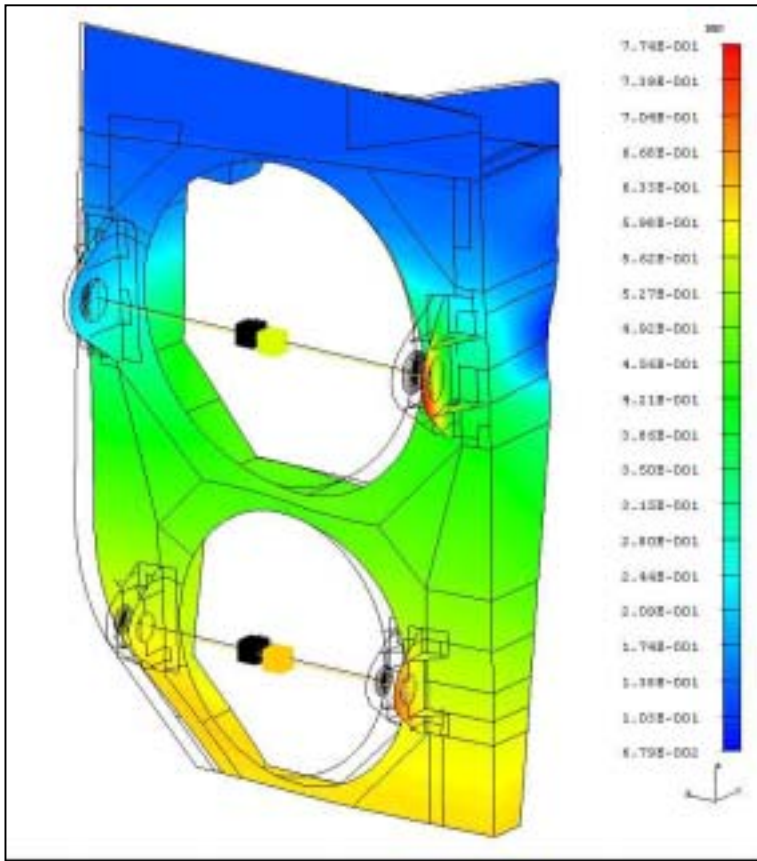


Fig.19 Plate Displacement (Lower Bracket and Helicoidal Spring hidden); load case (3.25, 13, 3.25) g

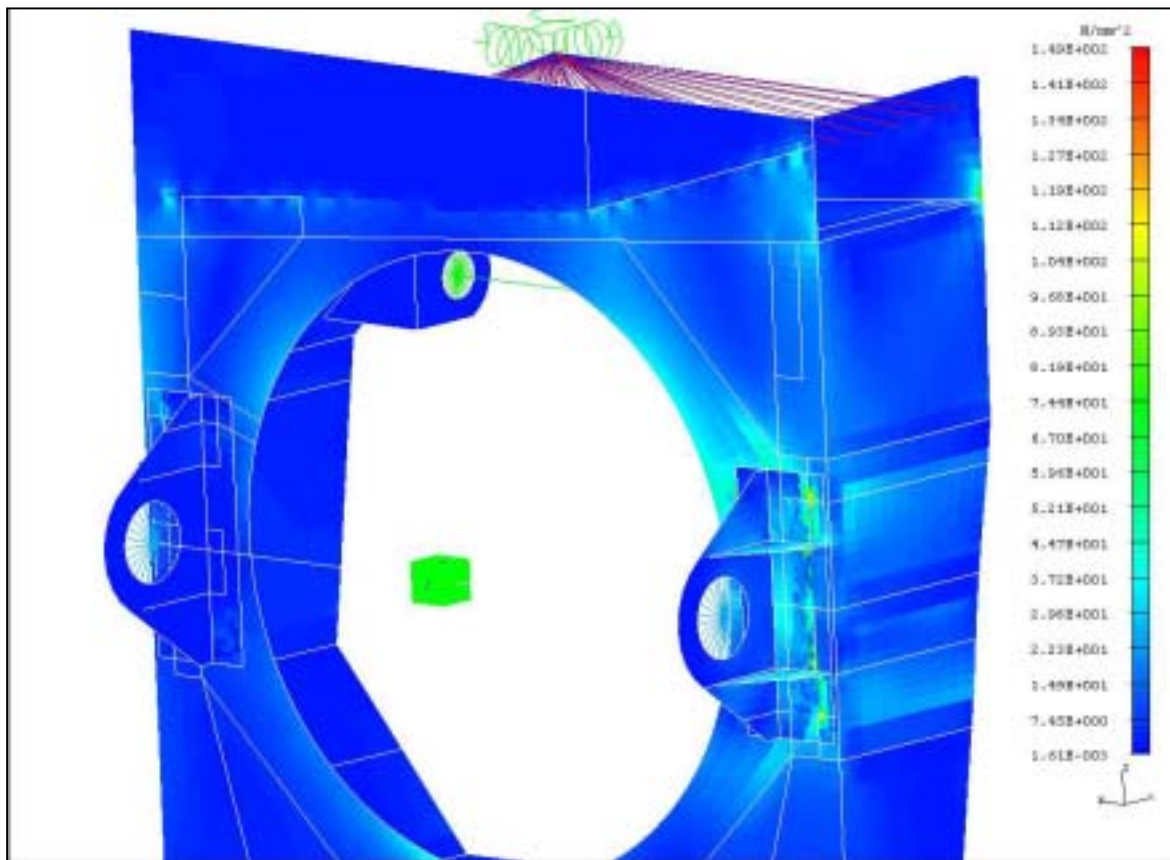


Fig.20 Plate Stress; load case (3.25, 13, 3.25) g

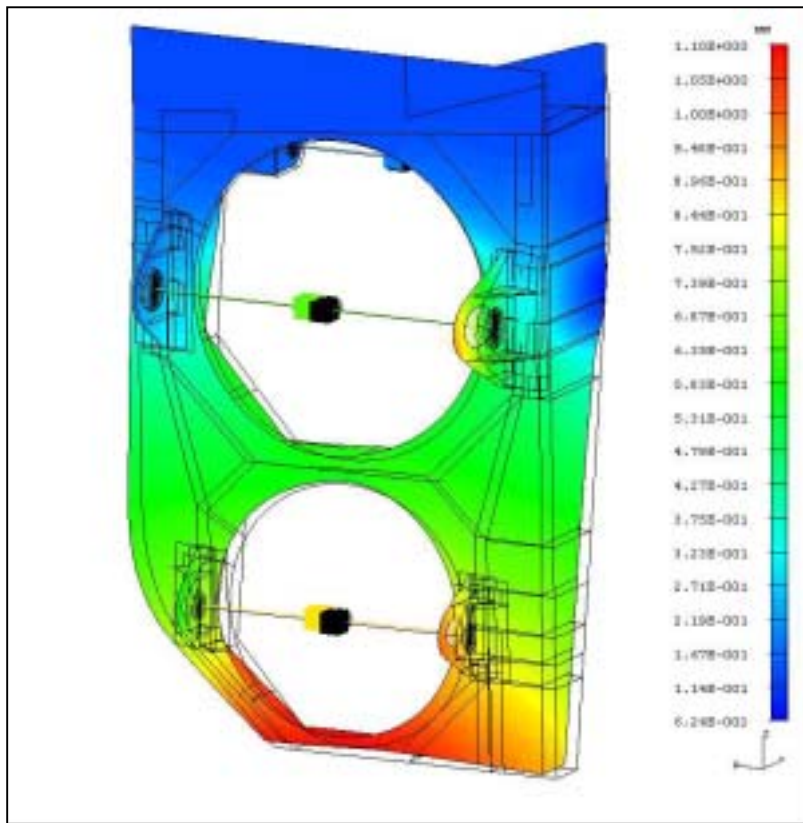


Fig.21 Plate Displacement (Lower Bracket and Helicoidal Spring hidden); load case (-3.25, -13, -3.25) g

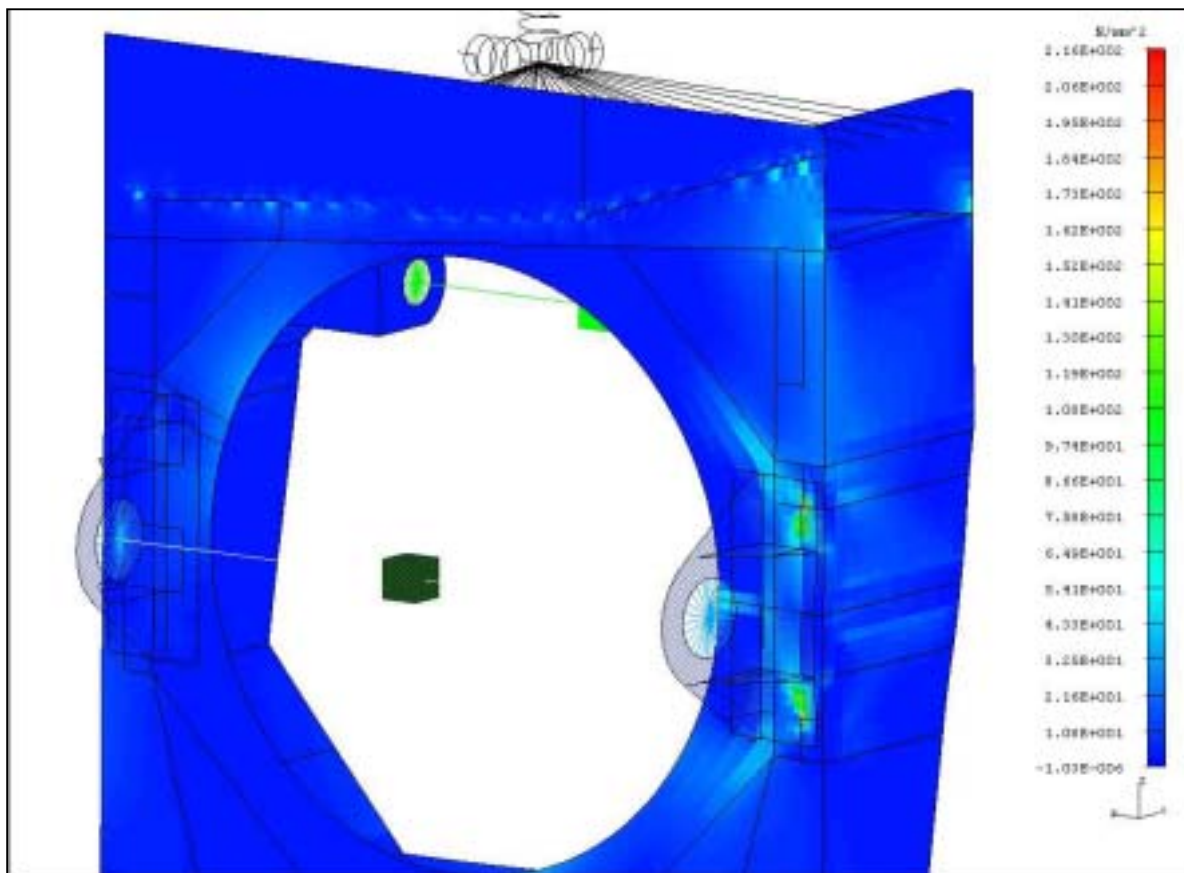


Fig.22 Plate Stress; load case (-3.25, -13, -3.25) g

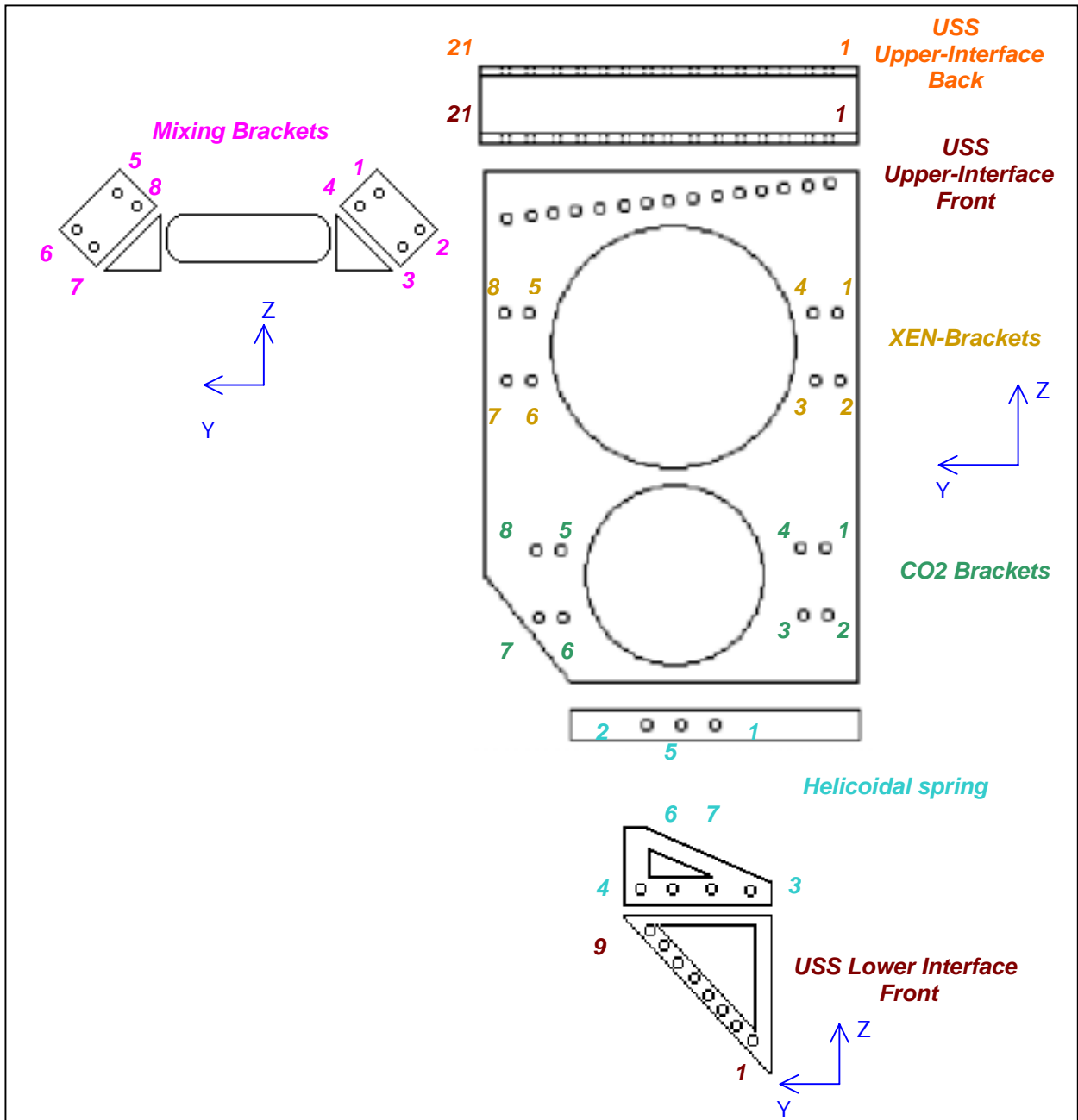


Fig.23 Bolts Analysis: bolts location

BOLTS ANALYSIS Load case: (13, 3.25, 3.25)g									
BOLT n°. (*)				TENSION [N]	SHEAR [N]	# BOLT	MARGIN OF SAFETY	#NUT #INSERT	MARGIN OF SAFETY
PLATE/	USS Upper Interface	BACK	21	-696.0	2962.6	NAS1954 .25-28	0.405	NAS1789	0.805
		BACK	1	-53.9	1861.5	NAS1954 .25-28	0.707	NAS1789	0.805
	XEN Bracket		4	2720.0	830.3	NAS1351 .375-24	0.979	NASM 14222	0.111
	CO2 Bracket		4	315.0	102.9	NAS1351 .315-24	0.909	NASM 14222	0.715
	Mixing Bracket		1	99.7	769.6	NAS1351 .25-28	0.657	MS 1209	1.371
	Helicoidal spring		1	-393.0	295.5	NAS1351 .25-28	0.674	NASM 14222	0.712
LOWER BRACKET/	Helicoidal spring		3	-448.0	325.0	NAS1351 .25-28	0.673	MS 1209	1.379
	USS Lower Interface	FRONT	1	-117.0	671.1	NAS1954 .25-28	1.399	MS 1209	1.428

BOLTS ANALYSIS Load case: (-13, -3.25, -3.25)g									
BOLT n°. (*)				TENSION [N]	SHEAR [N]	# BOLT	MARGIN OF SAFETY	#NUT #INSERT	MARGIN OF SAFETY
PLATE/	USS Upper Interface	BACK	21	787.0	3583.4	NAS1954 .25-28	0.242	NAS1789	0.769
		BACK	1	66.7	2777.1	NAS1954 .25-28	0.454	NAS1789	0.802
	XEN Bracket		1	521.0	1166.4	NAS1351 .375-24	1.023	NASM 14222	0.139
	CO2 Bracket		2	60.8	161.3	NAS1351 .315-24	0.918	NASM 14222	0.725
	Mixing Bracket		1	-116.7	983.5	NAS1351 N4.25-28	0.649	MS 1209	1.379
	Helicoidal Spring		1	-204.0	661.6	NAS1351 .25-28	0.666	NASM 14222	0.712
LOWER BRACKET/	Helicoidal spring		3	-275.0	493.3	NAS1351 .25-28	0.671	MS 1209	1.379
	USS Lower Interface	FRONT	1	-25.5	516.9	NAS1954 .25-28	1.416	MS 1209	1.428

BOLTS ANALYSIS Load case: (3.25, 13, 3.25)g									
BOLT n°. (*)				TENSION [N]	SHEAR [N]	#BOLT	MARGIN OF SAFETY	#NUT #INSERT	MARGIN OF SAFETY
PLATE/	USS Upper Interface	FRONT	1	-10.4	3771.8	NAS1954 .25-28	0.206	NAS1789	0.805
		FRONT	21	96.7	2963.8	NAS1954 .25-28	0.403	NAS1789	0.801
	XEN Bracket		4	4540.0	3727.3	NAS1351 .375-24	0.816	NASM 14222	0.088
	CO2 Bracket		3	710.0	213.9	NAS1351 .315-24	0.894	NASM 14222	0.7
	Mixing Bracket		2	-99.0	352.5	NAS1351 .25-28	0.673	MS 1209	0.712
	Helicoidal Spring		1	-522.0	347.1	NAS1351 .25-28	0.673	NASM 14222	0.712
LOWER BRACKET/	Helicoidal spring		3	-587.0	363.5	NAS1351 .25-28	0.673	MS 1209	1.379
	USS Lower Interface	FRONT	1	-46.1	671.8	NAS1954 .25-28	1.399	MS 1209	1.428

BOLTS ANALYSIS Load case: (3.25, 3.25, 13)g									
BOLT n°. (*)				TENSION [N]	SHEAR [N]	#BOLT	MARGIN OF SAFETY	#NUT #INSERT	MARGIN OF SAFETY
PLATE /	USS Upper Interface	FRONT	21	108.0	2408.3	NAS1954 .25-28	0.556	NAS1789	0.800
		FRONT	20	64.3	1505.6	NAS1954 .25-28	0.789	NAS1789	0.802
	XEN Bracket		4	2140.0	2740.4	NAS1351 .375-24	0.932	NASM 14222	0.118
	CO2 Bracket		4	254.0	233.0	NAS1351 .315-24	0.911	NASM 14222	0.717
	Mixing Bracket		5	216.2	91.6	NAS1351 .25-28	0.664	NASM 14222	0.700
	Helicoidal spring		1	-369.0	447.5	NAS1351 .25-28	0.672	NASM 14222	0.712
LOWER BRACKET/	Helicoidal spring		3	-444.0	403.3	NAS1351 .25-28	0.672	MS 1209	1.379
	USS Lower Interface	FRONT	1	-81.4	739.7	NAS1954 .25-28	1.388	MS 1209	1.428

(*) ref. Fig.23

Table 3 Bolts Analysis:
Bolts Tensile, Shear forces and Margin of Safety under different load cases [N]

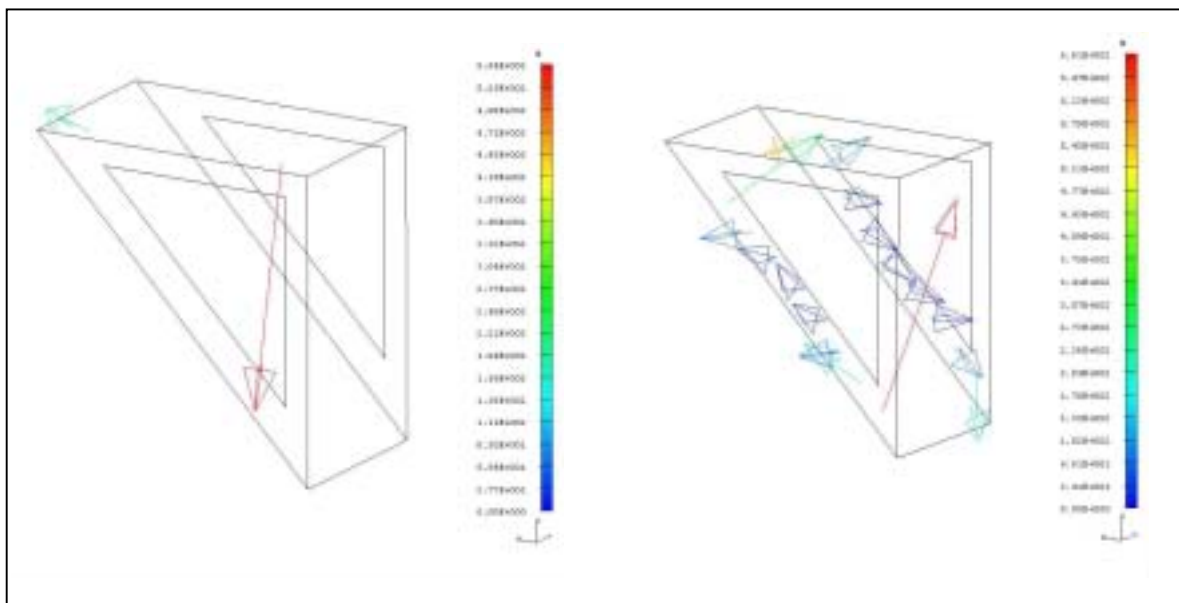
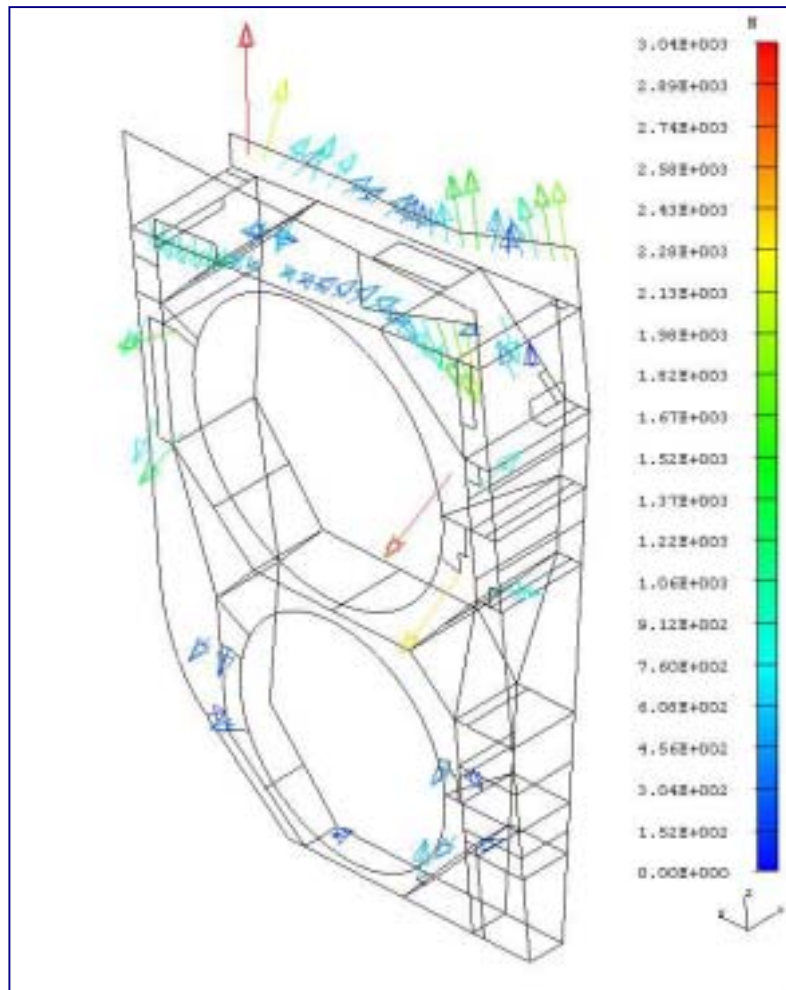


Fig.24 Plate and Lower Bracket Reactions; load case (13, 3.25, 3.25) g

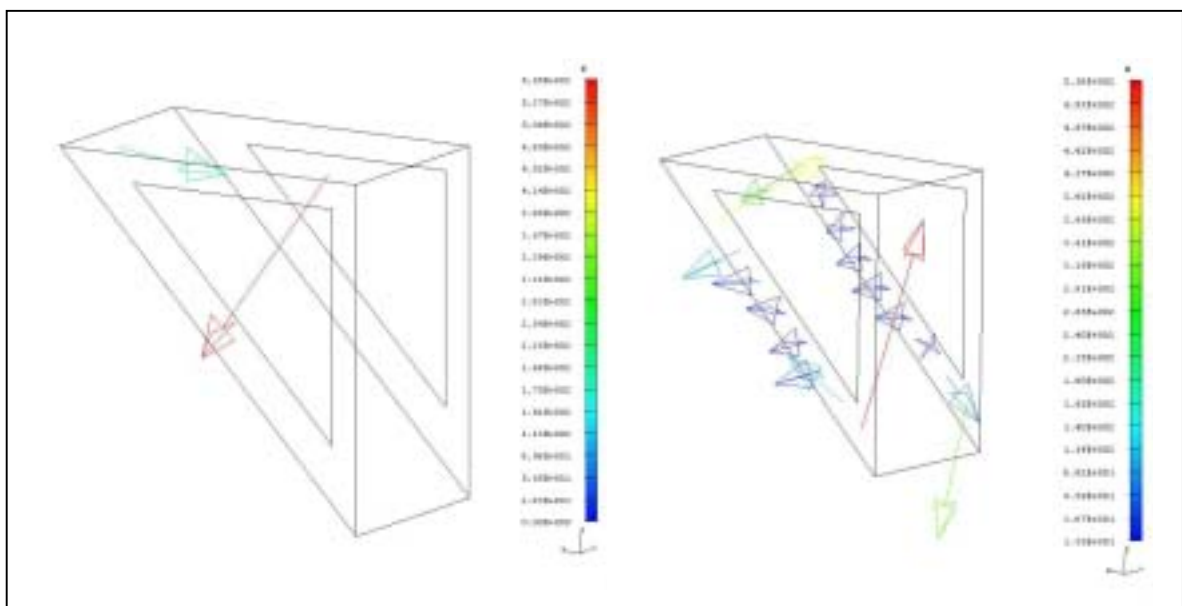
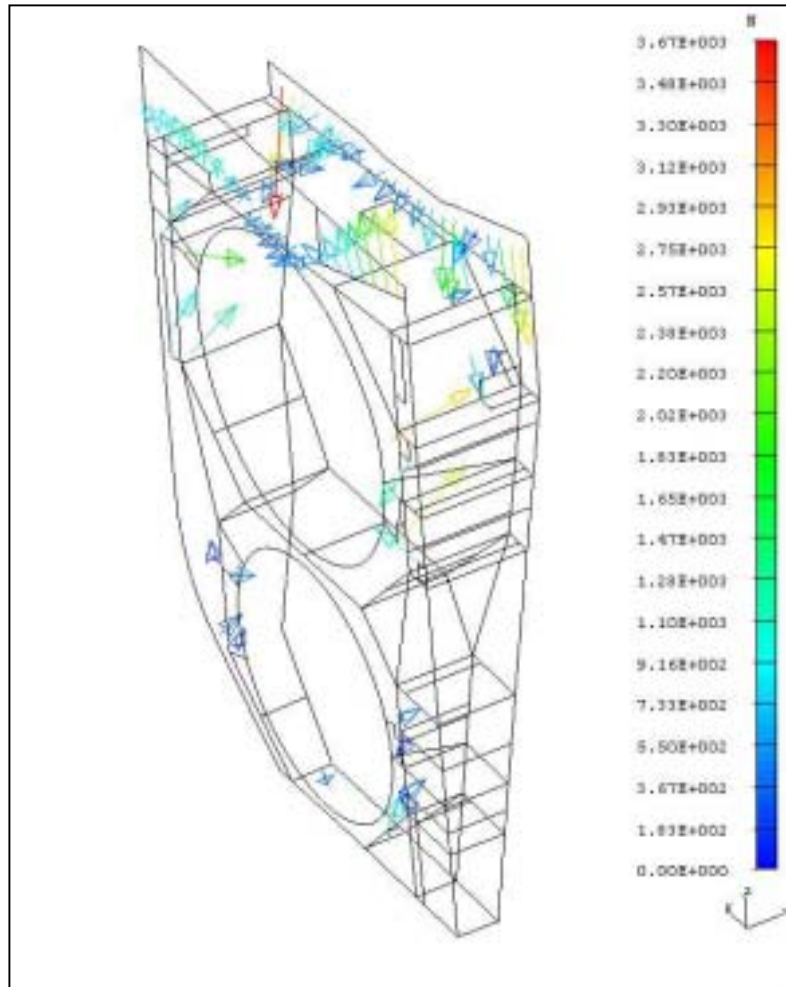


Fig.25 Plate and Lower Bracket Reactions; load case (-13, -3.25, -3.25) g

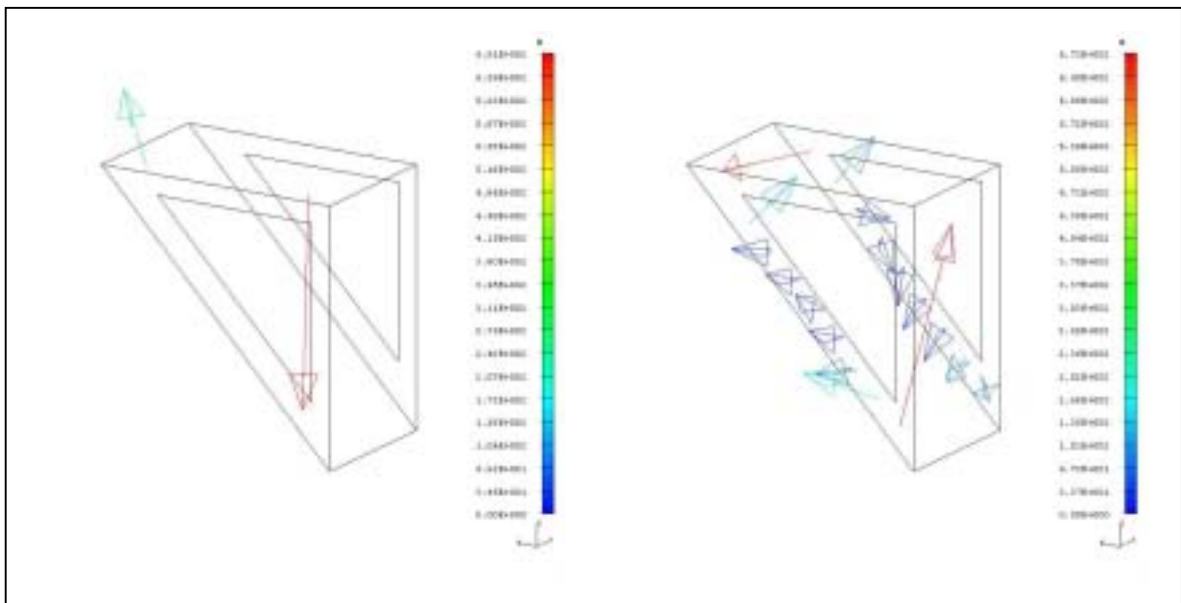
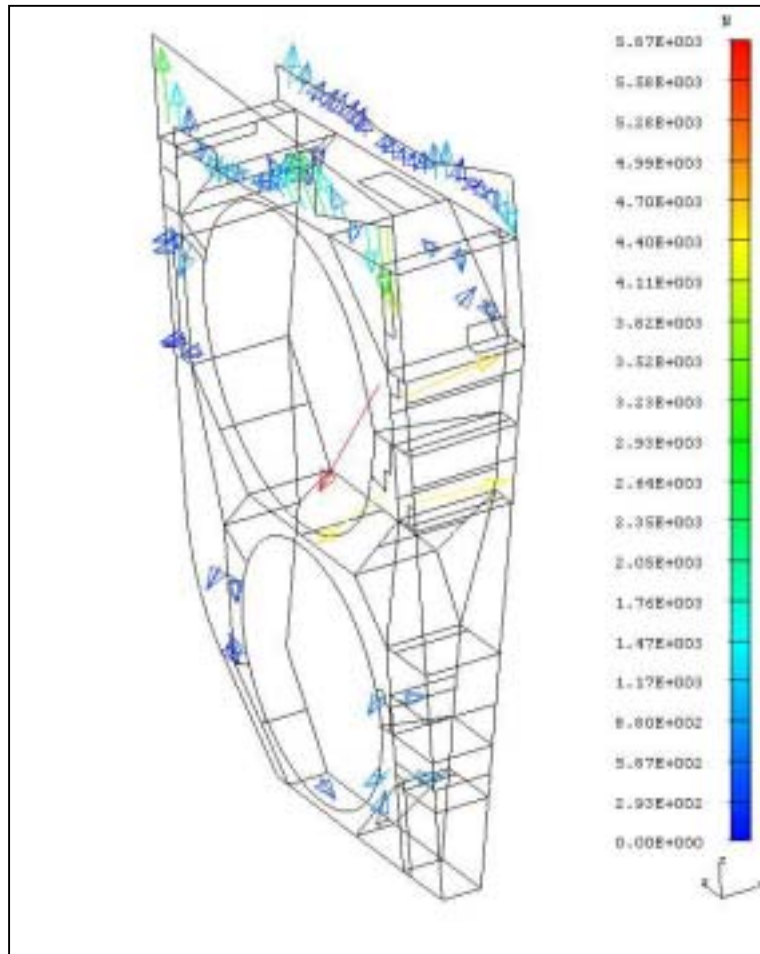


Fig.26 Plate and Lower Bracket Reactions; load case (3.25, 13, 3.25) g

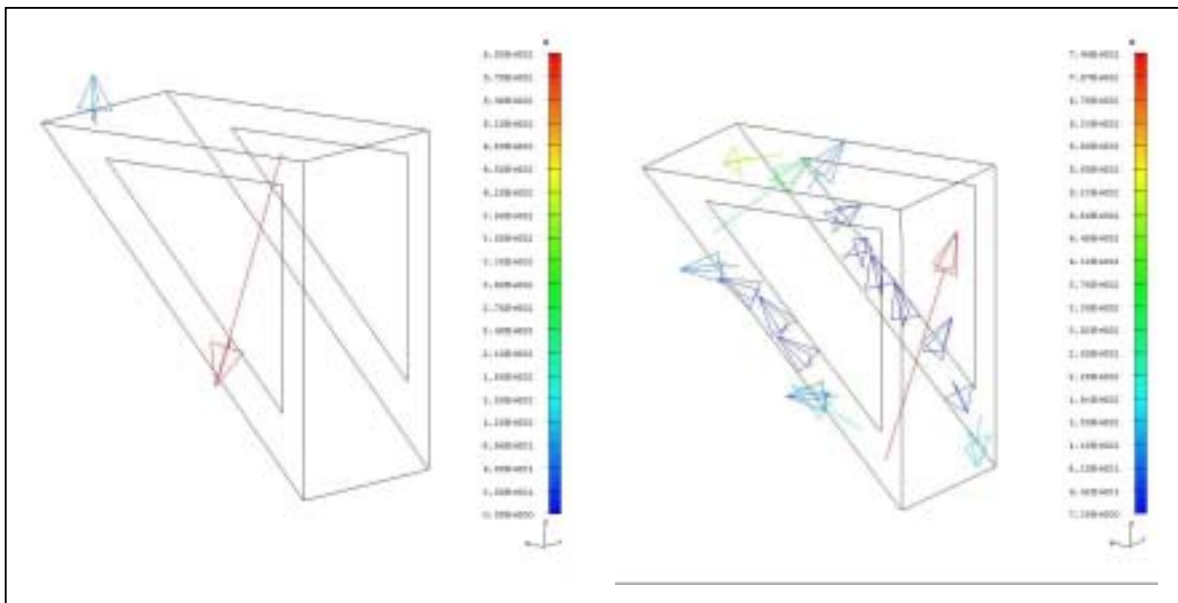
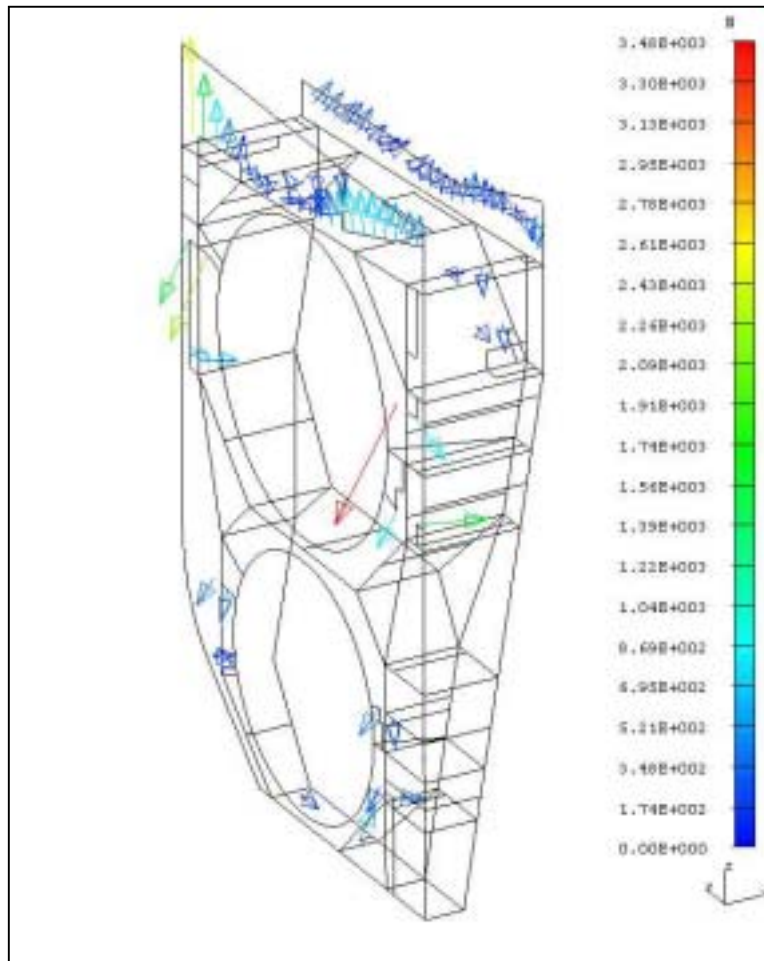


Fig.27 Plate and Lower Bracket Reactions; load case (3.25, 3.25, 13) g

FAIL SAFE ANALYSIS							
LOADS:			PLATE				
Acceleration (g)			BOLT Removed no.(*)	Limit Stress [N/mm ²]		Margin of Safety	
x	y	z		Von Mises	Max Principal	Yield	Ultimate
-13	-3.25	-3.25	PLATE/ USS Upper Interface BACK 21	184	136	1.10	2.35
3.25	13	3.25	PLATE/ Xen Bracket 4	193	131	1.00	2.47
			PLATE/ USS Upper Interface FRONT 1	153	123	1.52	2.70

FAIL SAFE ANALYSIS							
LOADS:			Lower BRACKET				
Acceleration (g)			BOLT Removed no.(*)	Limit Stress [N/mm ²]		Margin of Safety	
x	y	z		Von Mises	Max Principal	Yield	Ultimate
-13	-3.25	-3.25	PLATE/ USS Upper Interface BACK 21	45.2	45	7.54	9.07

**Table 4 Fail Safe Analysis:
Stress and Margin of Safety
under different load cases in critical components**

BOLTS FAIL SAFE ANALYSIS								
Load case	BOLT Removed no.(*)	BOLT no.(*)	TENSILE [N]	SHEAR [N]	#BOLT	MARGIN OF SAFETY	#NUT #INSERT	MARGIN OF SAFETY
-13, -3.25, -3.25	PLATE/ USS Upper Interface BACK 21	PLATE/ USS Upper Interface BACK 20	895	6396	NAS1954 .25-28	0.378	NAS1789	2.568
3.25, 13, 3.25	PLATE/ Xen Bracket 4	PLATE/ Xen Bracket 1	7640	1980.89	NAS 1351 .375-24	1.006	NAS1351	1.194
	PLATE/ USS Upper Interface FRONT 1	PLATE/ USS Upper Interface FRONT 2	13.4	5666.61	NAS1954 .25-28	0.49	NAS1789	2.61
3.25, 3.25, 13	Lower Bracket/ USS Lower Interface FRONT 1	Lower Bracket/ USS Lower Interface FRONT 2	42.9	181.08	NAS1954 .25-28	1.676	MS1209	3.852

**Table 5 Fail Safe Bolts Analysis:
Bolts Tensile, Shear forces and Margin of Safety
under different load cases**

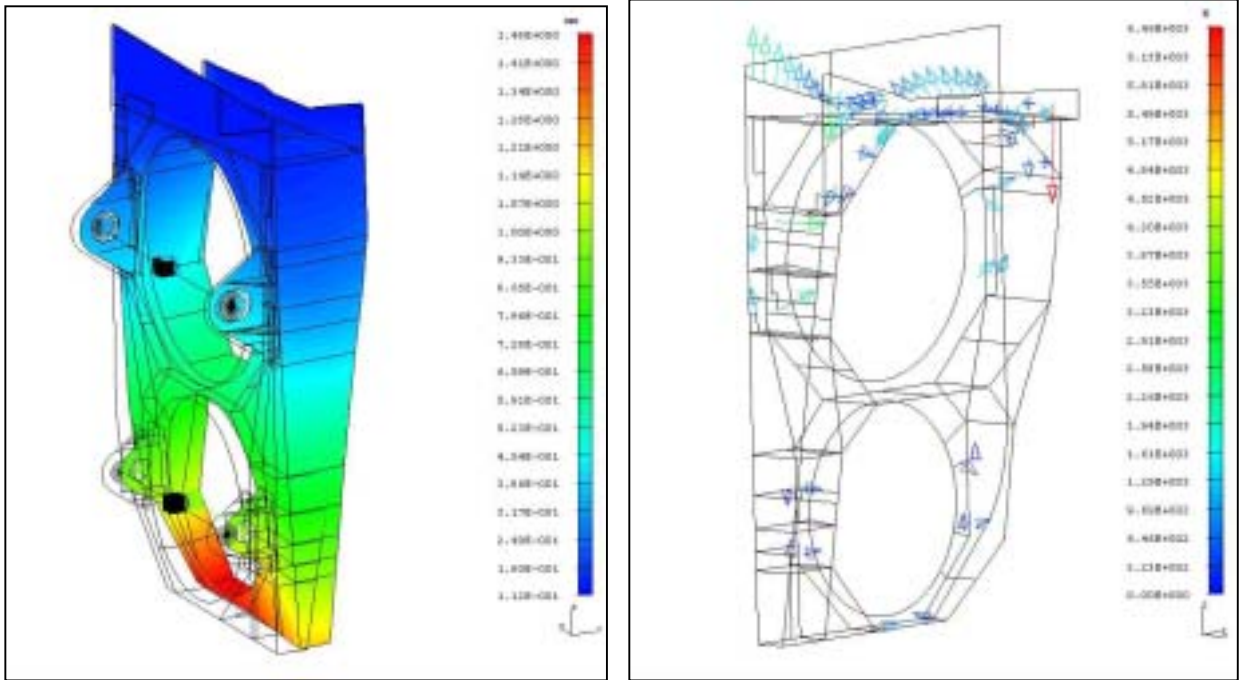


Fig.28 Fail Safe Analysis:
Plate Displacement and Reactions; load case (-13, -3.25, -3.25) g
Bolt removed: Plate/USS_upper_interface_back_21
Fig.29 Fail Safe Analysis:

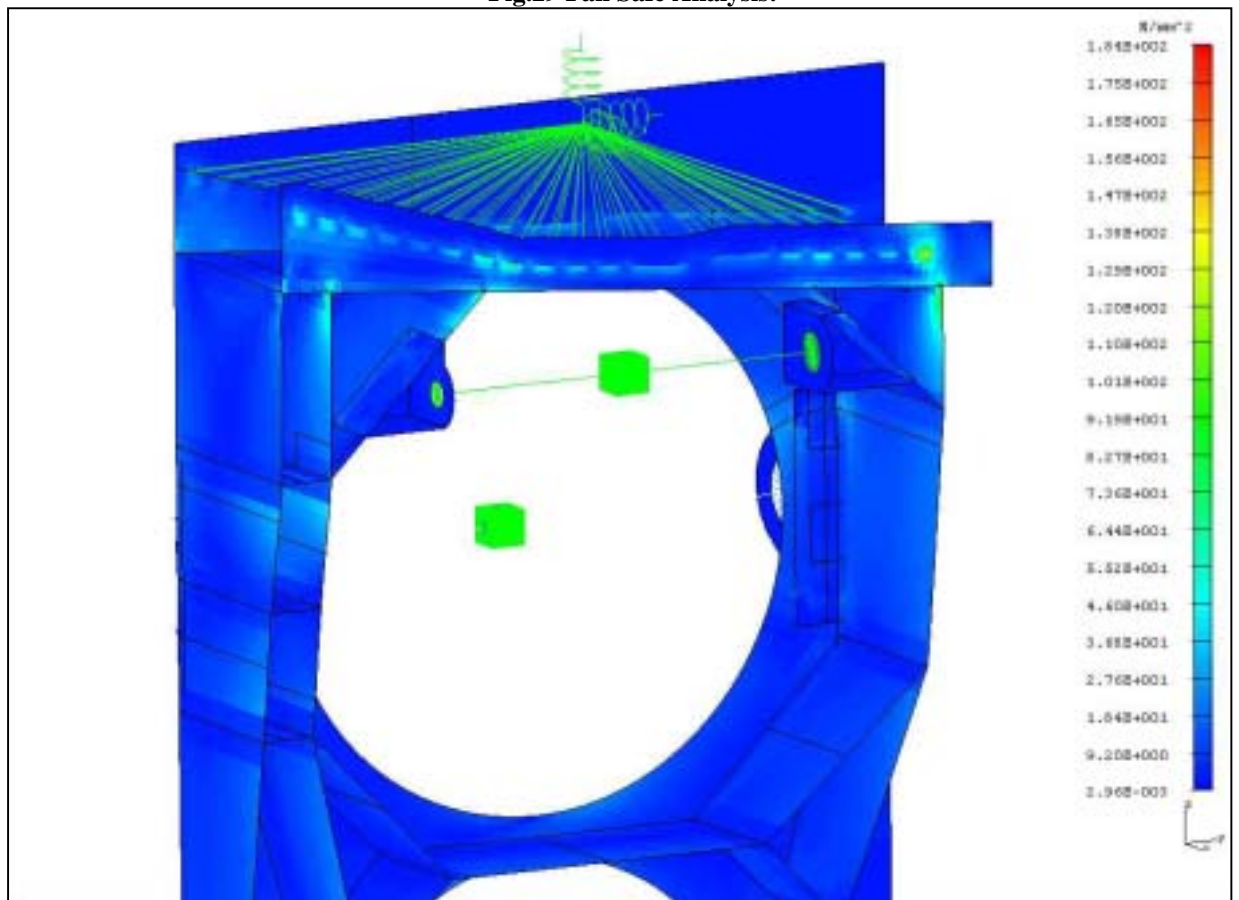


Plate Stress; load case (-13, -3.25, -3.25) g
Bolt removed: Plate/USS_upper_interface_back_21

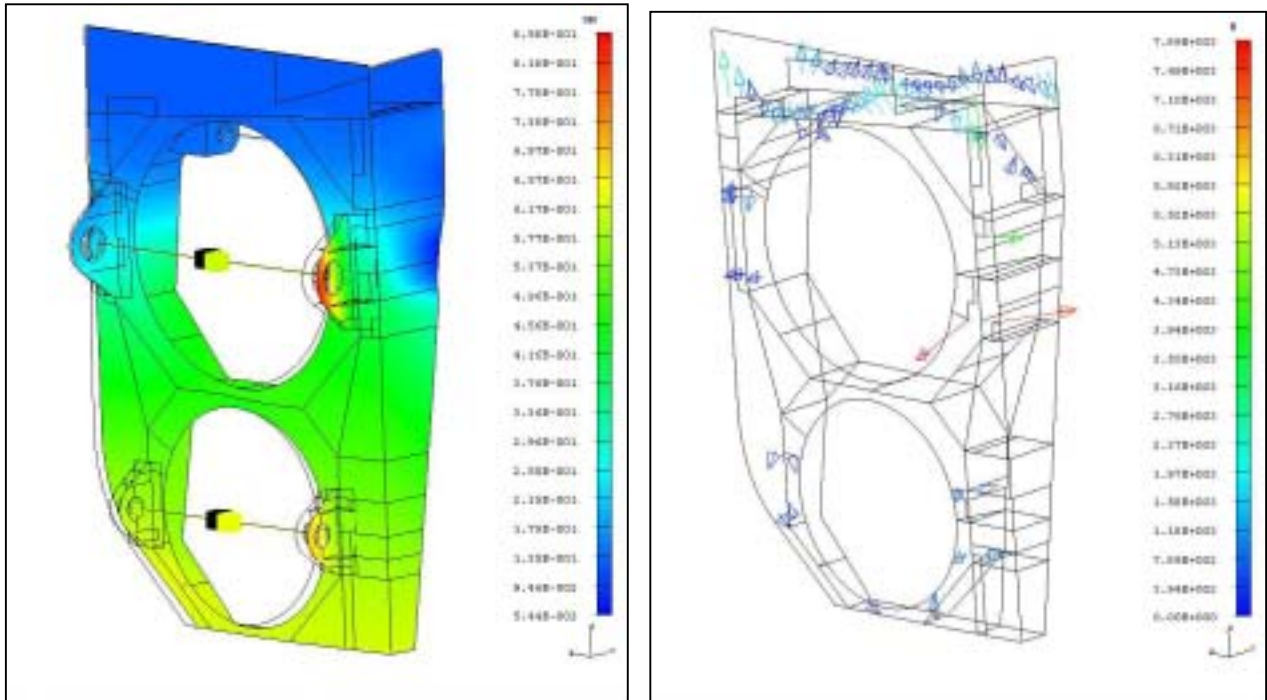


Fig.30 Fail Safe Analysis:
Plate Displacement and Reactions; load case (3.25, 13, 3.25) g
Bolt removed:Plate/Xen_bracket_4

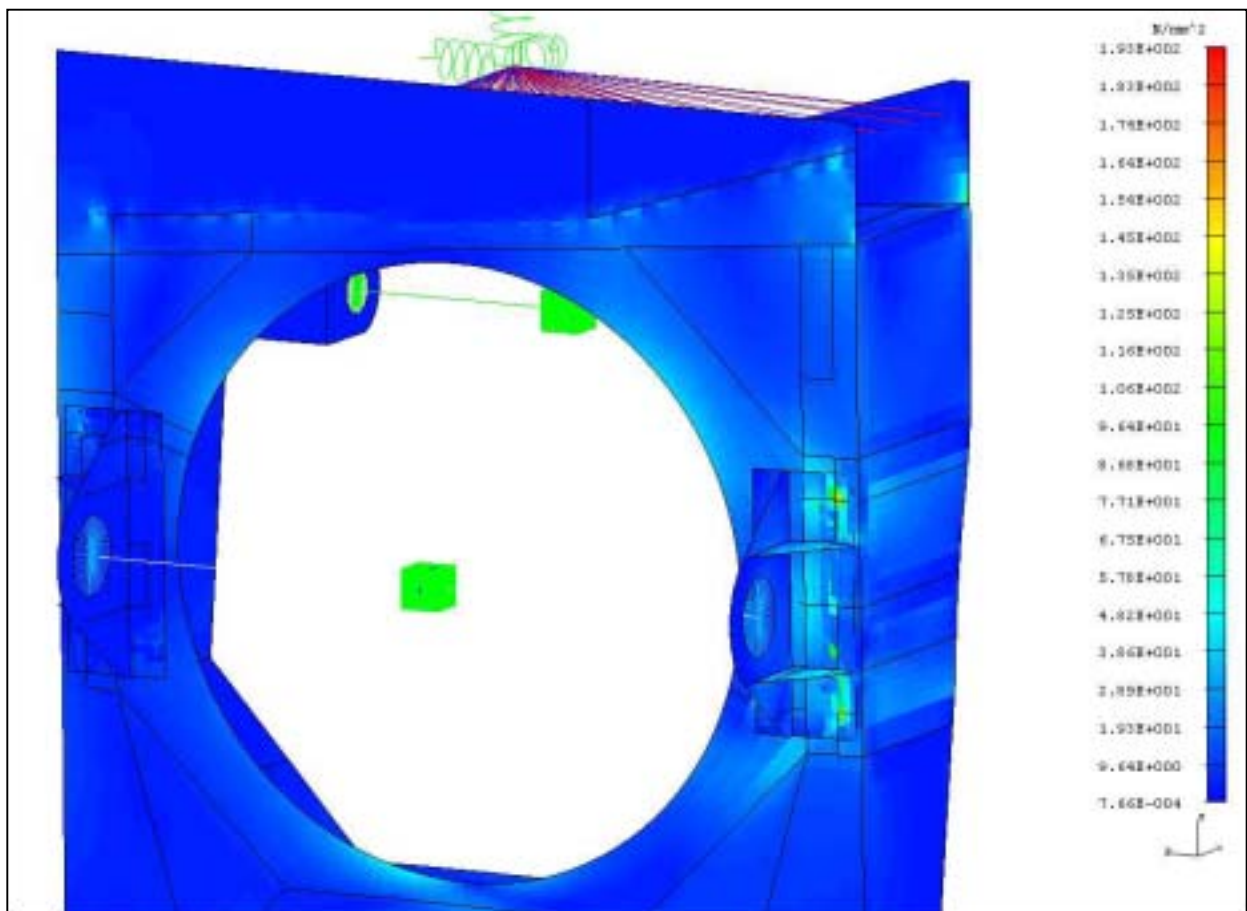


Fig.31 Fail Safe Analysis:
Plate Stress; load case (3.25, 13, 3.25) g
Bolt removed:Plate/Xen_bracket_4

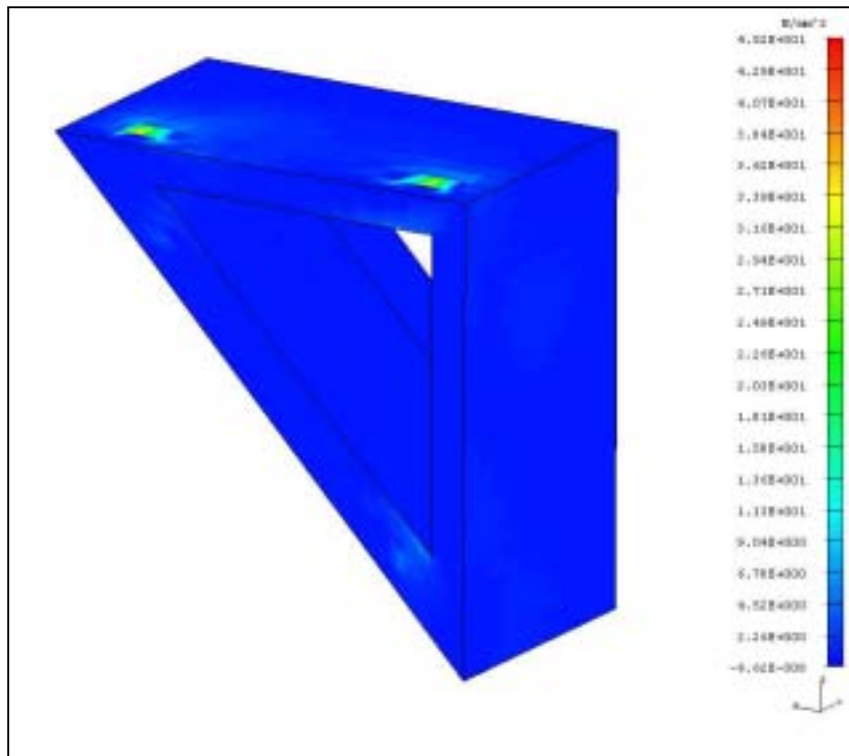


Fig.32 Fail Safe Analysis:
Lower Bracket Stress (3.25, 3.25, 13) g
Bolt removed:Lower_bracket/USS_lower_interface_front_1

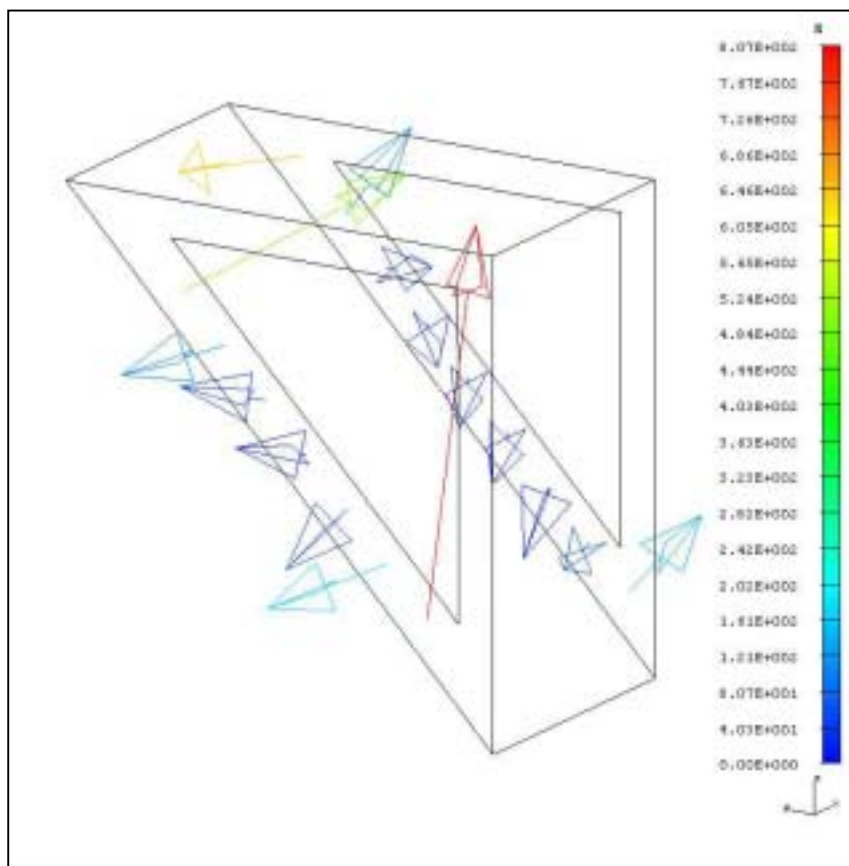


Fig.33 Fail Safe Analysis:
Lower Bracket Reactions, load case (3.25, 3.25, 13) g
Bolt removed:Lower_bracket/USS_lower_interface_front_1

§3.8. Modal Analysis:

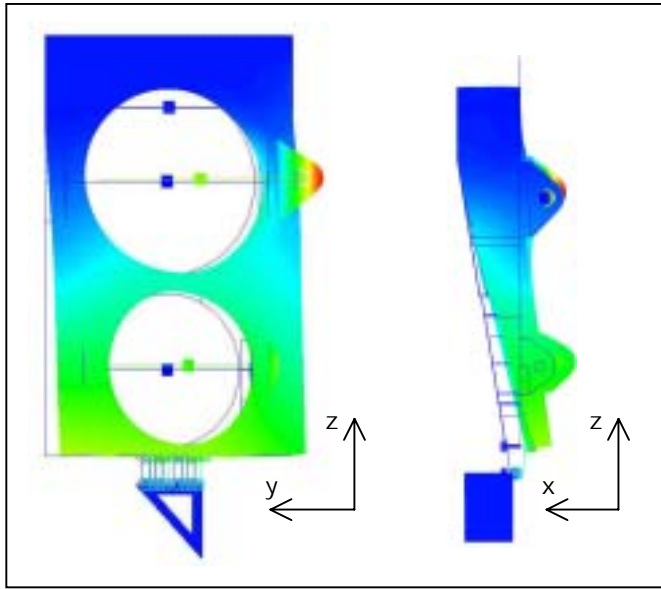


Fig 34 Previous Analysis: First Mode 64

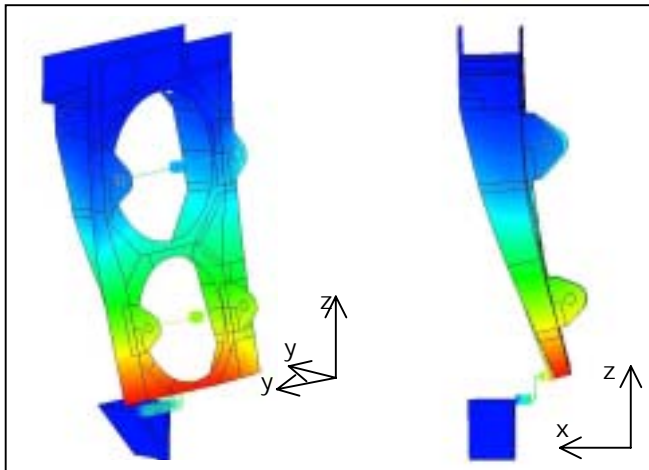


Fig 35 Previous Analysis: Second Mode 74 Hz

For the Modal Analysis a normal mode dynamics Lanczos Method was applied.

Previous analysis predicted a first local mode at Xe bracket level associated to Xe tank mass participation in the axial direction (fig 34,35, tab.3).

The introduction of the final stiffer bracket geometry in the FE model and a stiffening of the plate area that support the main brackets by adding a rib, produced a raise of the frequency of the local mode from 64 Hz to 88 Hz.

Fig.36 and 37 show the positive effect of the area stiffening on the first mode by comparing previous to actual analysis.

Then first mode occurs at the natural frequency of 74 Hz with a bending modal shape in the x direction, while the local mode at bracket level shift to the second mode 88 Hz (fig.38, 39).

The first ten modes natural frequencies and effective normalized masses (participating mass/total mass) are listed in tab.5.

First mode natural frequency satisfies structural requirements (1st mode > 50Hz)

A sine sweep test for experimental evaluation of the real final system natural frequencies will be performed.

Mode	Frequency (Hz)	Normalized effective mass		
		x	y	z
1	64.29	0.0331	0.7258	0.004365
2	74.16	0.2743	0.0667	0.03178
3	95.04	0.0045	0.0284	0.0012

Table 4 Previous Analysis: first three modes

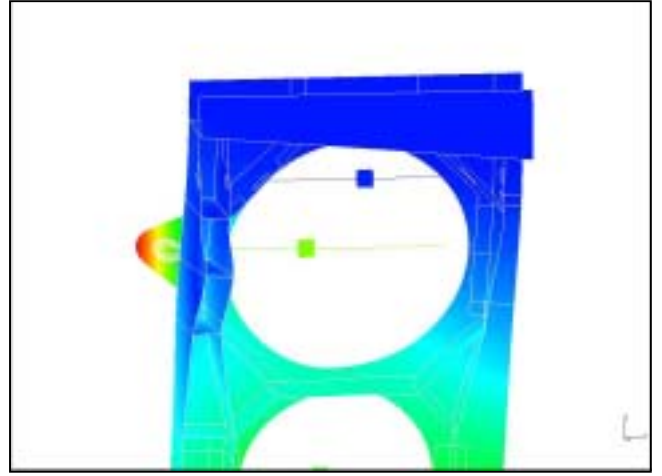
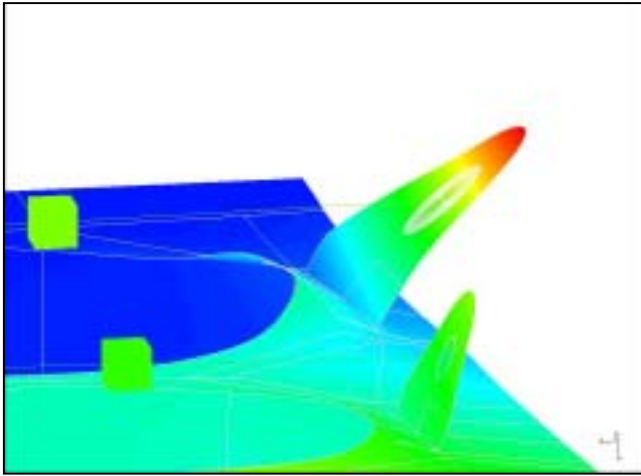


Fig 36 Previous Analysis: First Mode 64 Hz

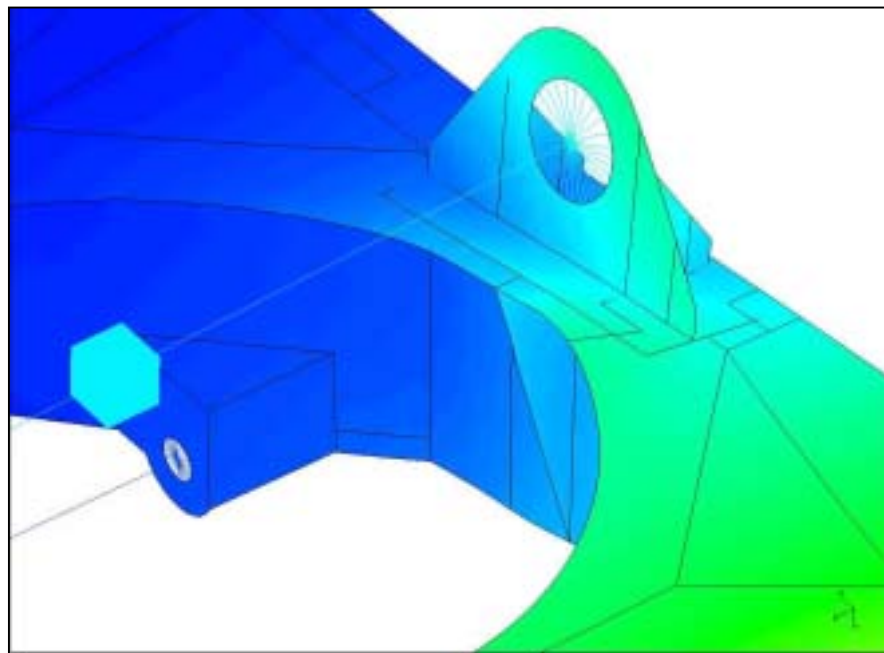


Fig 37 Actual Analysis: First Mode 74 Hz, stiffer Bracket area

Mode	Frequency (Hz)	Normalized effective mass		
		x	y	z
1	74.023	0.2701	0.14496	0.0254
2	87.867	0.0414	0.6649	0.0050
3	109.84	0.1160	0.0009	0.0003
4	126.06	0.0153	0.0050	0.0037
5	148.76	0.00187	0.0010	0.0030
6	169.02	0.0022	0.0000	0.0005
7	177.99	0.1218	0.0020	0.0001
8	204.05	0.2444	0.0042	0.0065
9	217.41	0.00943	0.0221	0.0337
10	256.74	0.04478	0.0000	0.0038

Table 5 Actual Analysis: First 10 Modes

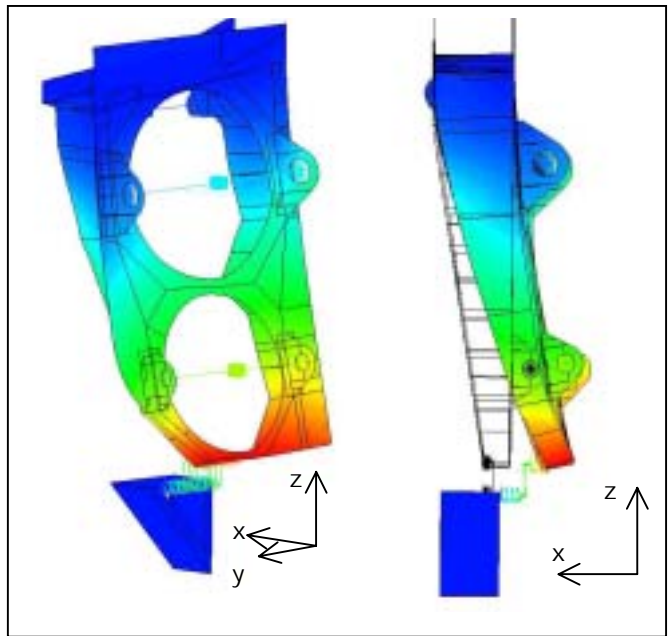


Fig 38 Actual Analysis: First Mode 74 Hz

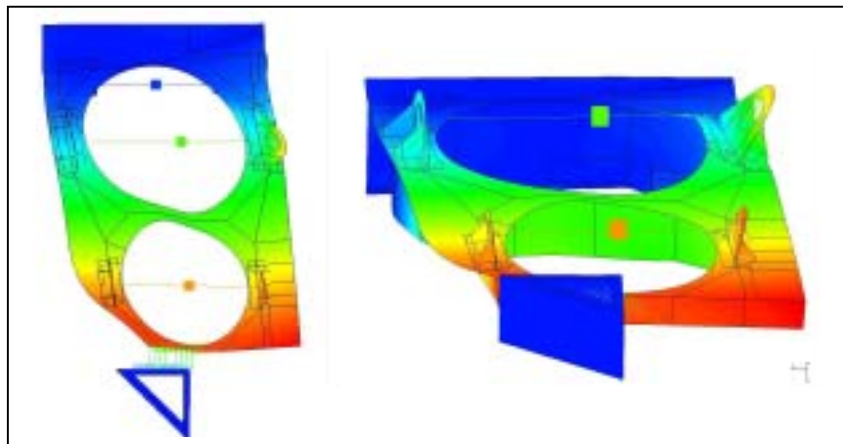


Fig 39 Actual Analysis: Second Mode 88 Hz

AMS TRD GAS SUPPLY SYSTEM BOX_S Mechanical Structure



Corrado Gargiulo INFN Roma
Robert Becker MIT



AMS Rome

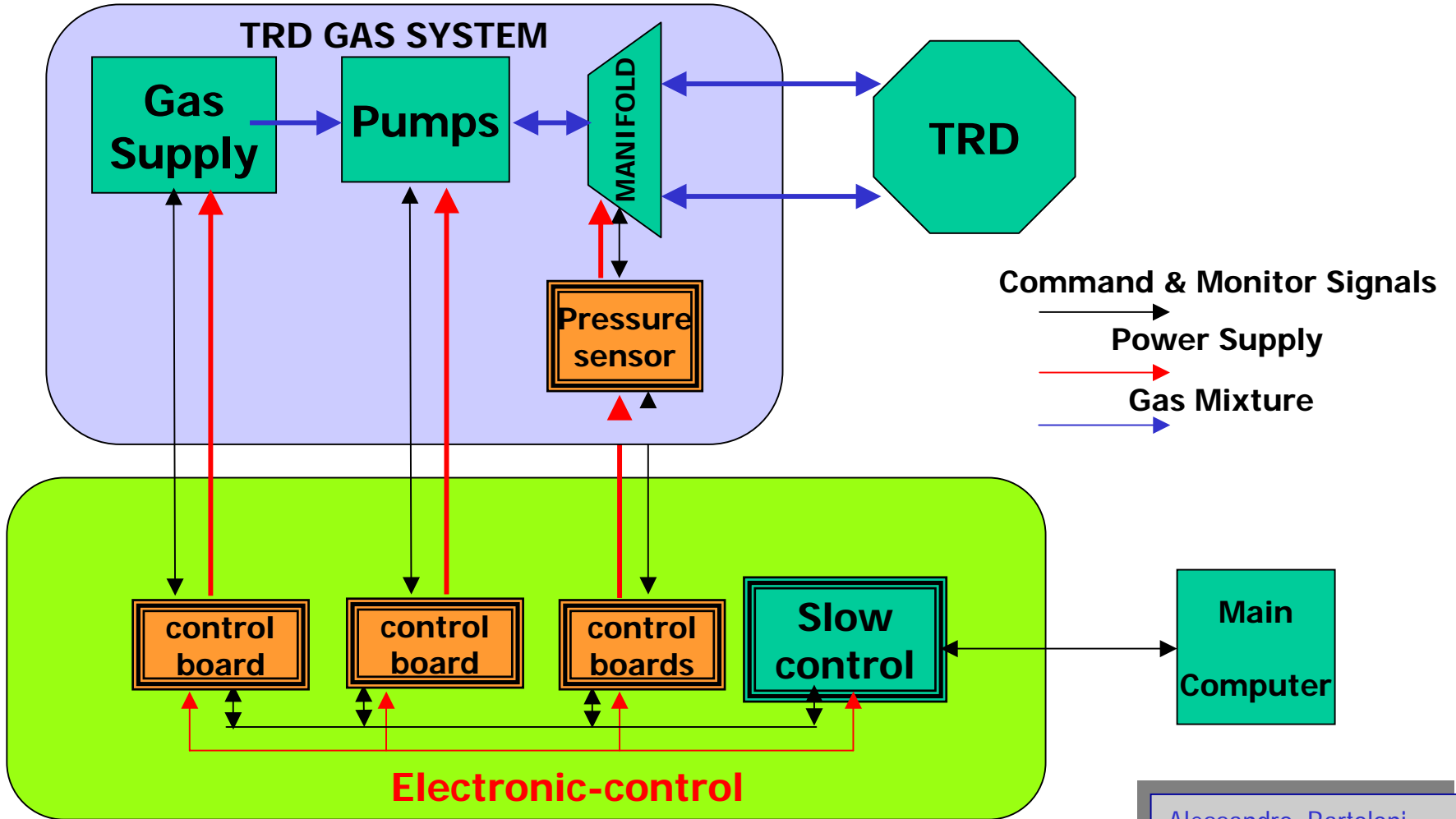
AMS TRD GAS SUPPLY SYSTEM ELECTRONIC CONTROL

To reach proton / positrons
rejection factor 10^{-3} :

Gas gain controlled
better than 1%.

Electronic design of gas control system and monitor
INFN Rome

AMS TRD GAS SYSTEM ELECTRONIC CONTROL



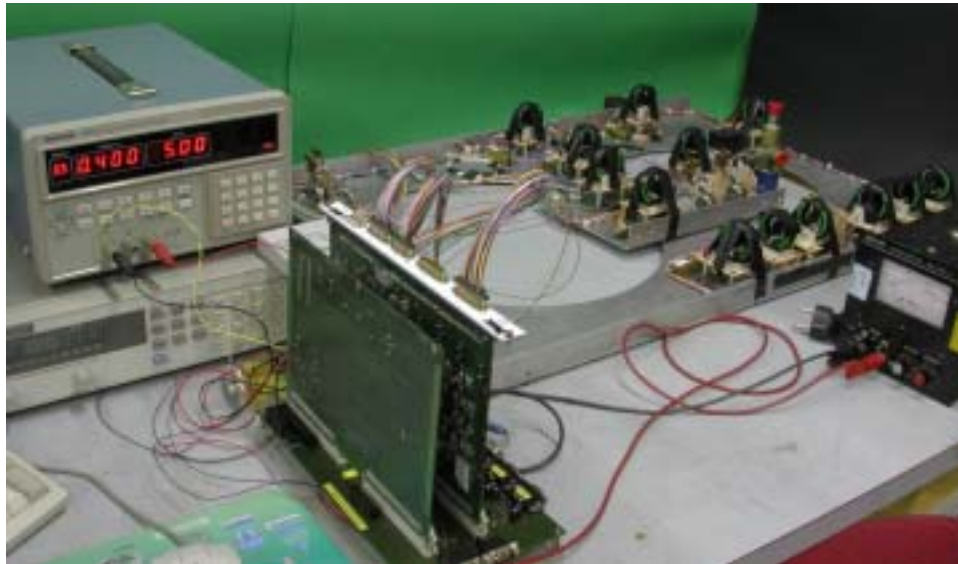


AMS Rome

AMS TRD GAS SYSTEM ELECTRONIC CONTROL

Engineering Electronic Boards ready and tested

Flight Boards ready summer 2003



AMS TRD GAS SYSTEM ELECTRONIC CONTROL

